VESTIBULAR PERCEPTION IN ADOLESCENTS WITH IDIOPATHIC SCOLIOSIS

by

Emma Jean Woo
B.H.K., The University of British Columbia, 2014

A THESIS SUBMITTED IN PARTIAL FULFILLMENT OF THE REQUIREMENTS FOR THE DEGREE OF

MASTER OF SCIENCE
in
THE FACULTY OF GRADUATE AND POSTDOCTORAL STUDIES
(Kinesiology)

THE UNIVERSITY OF BRITISH COLUMBIA
(Vancouver)

July 2018

The following individuals certify that they have read, and recommend to the Faculty of Graduate and Postdoctoral Studies for acceptance, a thesis/dissertation entitled:

Vestibular perception in adolescents with idiopathic scoliosis

submitted by Emma Woo in partial fulfillment of the requirements for

the degree of Master of Science

in Kinesiology

Examining Committee:

Jean-Sébastien Blouin, PhD, DC
Supervisor

Gunter P. Siegmund, PhD, PEng
Supervisory Committee Member

Christopher W. Reilly, MD, FRCSC
Supervisory Committee Member

Abstract

Adolescent Idiopathic Scoliosis (AIS) is a three-dimensional spinal deformity. One of the proposed causes of AIS is asymmetric vestibular function and the related descending drive to the spine musculature. Indeed, unilateral labyrinthectomy in tadpoles results in a spinal curvature similar to scoliosis. The objective of this study was to determine if asymmetric vestibular function is present in individuals with AIS. Ten individuals with AIS (8 females, 2 males) and ten healthy controls (8 females, 2 males) were exposed to 10s virtual rotations induced by monaural or binaural electrical vestibular stimulation (EVS), and 10s real rotations delivered by sitting atop a rotary chair. Using a forced-choice paradigm, participants indicated their perceived rotation direction (right or left). A Bayesian adaptive algorithm adjusted the stimulus intensity and direction to identify a stimulus level, which we called the vestibular recognition threshold, at which participants correctly identified the rotation direction 69% of the time. For unilateral vestibular stimuli (monaural EVS), the recognition thresholds were more asymmetric in all participants with AIS compared to control participants (1.16 vs 0.06 mA; $p < 0.001$) but the recognition thresholds for bilateral vestibular stimuli did not differ between groups for both real and virtual rotations (multiple $p > 0.05$). No correlation was observed between the degree/side of the spine curvature and vestibular asymmetry in persons with AIS ($p = 0.30$). Our results demonstrate an asymmetry in vestibular function in individuals with AIS. Previous reports of semicircular canal orientation asymmetry in individuals with AIS could not explain this vestibular function asymmetry, suggesting a functional cause of the observed vestibular asymmetry. Vestibular function related to bilateral stimuli was well compensated, showing similar recognition thresholds across both groups of participants. The present results indicate that

vestibular dysfunction is linked to AIS, potentially revealing a new path for the screening and monitoring of scoliosis in adolescents.

Lay Summary

Adolescent idiopathic scoliosis (AIS) is a type of three-dimensional spinal deformity without a well-defined cause. Research in humans and animals suggests that individuals with AIS may have a vestibular dysfunction. The aim of this research was to determine if individuals with AIS have an asymmetric vestibular function. We assessed vestibular function by quantifying participants vestibular perception thresholds to real (chair) and virtual (evoked by electrical stimuli) rotations. Asymmetry in vestibular function was estimated by comparing virtual rotations applied unilaterally. The results showed that all participants with AIS exhibited an asymmetric unilateral vestibular function, characterized by a less sensitive function on one side. We propose that methodologies assessing unilateral vestibular function could lead to diagnostic tools with a high sensitivity and specify.

Preface

The protocol used in this study was reviewed by The University of British Columbia Clinical Research Ethics Board (UBC CREB: H16-00801). All participants provided written informed consent and assent prior to participation in these studies and every effort has been made to ensure that the participants are not identified in this thesis.

I was the lead investigator on the project, responsible for concept formation, data collection and analysis, and document composition. Dr. Jean-Sébastien Blouin was the supervisory author on the project and was involved in the concept formation, data analysis and thesis revisions. Dr. Gunter P. Siegmund was involved in concept development and thesis revisions. Dr. Christopher W. Reilly was involved in thesis revisions. The experiment in Chapter 2 will be submitted for scientific publication.

The statistical analysis was completed in JASP (v0.8.6, The JASP Team, The Netherlands) and the significance level was set at $\alpha < 0.05$.

Table of Contents

Lists of Tables

List of Figures

List of Equations

List of Abbreviations

AIS	Adolescent Idiopathic Scoliosis
BCCH	British Columbia Children's Hospital
Binaural	Binaural bipolar
Curvature	Major convex curvature
EMG	Electromyography
EVS	Electrical vestibular stimulation
IS	Idiopathic Scoliosis
MET	Mechanoelectric transduction
Monaural	Monaural bipolar
PVP	Position-vestibular-pause
SCEP	Somatosensory cortical evoked potentials
VEMP	Vestibular evoked myogenic potentials
VOR	Vestibular ocular response

Acknowledgements

I would first like to thank my supervisory committee. Thank you to Dr. Jean-Sébastien Blouin, who I was fortunate to be supervised and supported by, who provided me with the resources to succeed, challenged me to be inquisitive, and helped me achieve my goals during my time as his student. And another thank you to Dr. Gunter P. Siegmund, and Dr. Christopher W. Reilly for providing guidance, feedback, comments and thought-provoking conversations. Together, this thesis would not have been possible without your collective expertise and I am grateful for all the time you have spent developing my research skills.

I would also like to thank Dr. Ryan Peters for his contributions to the Bayesian algorithm. As well, I would like to thank Jiyu Wang for her contribution to the computational model. And thank you to Dr. Romain Tisserand for his continuous assistance reviewing documents, Matlab coding, and creating nice figures. And Dr. Chris McNeil, for helping me get my start in research and being a great mentor to me.

I would also like to thank the research assistants and nurses at BC Children's Hospital's Orthopedic Clinic, for all the time and assistance put in to help screen participant charts and recruit Individuals with AIS. And I would like to thank the schools that allowed me to speak to your students, as I would not have been able to complete my data collection without your help. I further thank all of the participants, and pilot participants, who made this research possible.

I would also like to thank all of the lab members in the Sensorimotor Physiology Lab for making the lab a great place to work, for all of your willingness to listen to my presentations, give thoughtful review and comments on this work, and general help with everything involved in the lab.

Finally, I would like to thank my friends and family. Your unwavering love and support has allowed me the opportunity to be successful.

Dedications

To my family

General Introduction

Scoliosis is the most common spinal deformity in humans. Many forms of scoliosis are idiopathic, meaning without a known cause. Adolescent idiopathic scoliosis (AIS) is the most common type of idiopathic scoliosis (IS), defined by a pathological onset between 10 and 16 years of age. Although the exact cause of IS remains unknown, studies indicate a multifactorial cause of IS that includes sensorimotor dysfunctions, one of which may be an asymmetric vestibular function.

The vestibular system encodes for head orientation and movement in space. Located bilaterally within the inner ears, both systems work in unison to receive and transmit signals of angular and linear acceleration. These signals of head orientation and movements drive ocular, spinal and appendicular musculature, but also contribute to higher-level cortical processing such as motion perception (Zwergal et al., 2009). Bilateral differences in encoding of head motion cues or integration of these cues by the vestibular system can result in functional vestibular asymmetry.

Vestibular asymmetry has been implicated as a potential factor contributing to the development of scoliosis. In tadpoles, unilateral removal of the vestibular system resulted in a spinal curvature that is similar to scoliosis in humans and persisted into adulthood (Lambert et al. 2009). While this study cannot possibly be replicated in humans, it is compelling evidence of asymmetric vestibular function being a potential causative factor in IS cases in humans. Asymmetric vestibular ocular response (VOR) was observed in Individuals with AIS with a right thoracic curvature in comparison to matched controls to unilateral vestibular stimulation (Sahlstrand et al., 1979a). Additionally, while standing, this stimulation evoked a greater lateral sway response in individuals with AIS (Sahlstrand et al., 1979b).

While this previous research has been promising in highlighting a potential link between AIS and vestibular function, these aforementioned studies, and others, have numerous limitations. Specifically, prior studies used caloric vestibular stimulation. Caloric vestibular stimulation mainly stimulates the horizontal semicircular canal within the peripheral vestibular system. Therefore, additional research is required to better understand vestibular function in individuals with AIS. Vestibular perception is a measure of vestibular function in human subjects (Merfeld, 2011). Thus, we sought to measure and compare vestibular recognition threshold to unilateral and bilateral vestibular stimuli in individuals with AIS and controls, in order to determine whether AIS have an asymmetrical perception to unilateral vestibular stimuli.

Vestibular perception can be evoked by using electrical vestibular stimulation (EVS). EVS artificially stimulates the vestibular system and can be used to elicit a perception of motion (Fitzpatrick et al., 2004; Peters et al., 2015). By orienting their head down, participants perceive a yaw rotation indistinguishable from a real motion of yaw rotation. Additionally, depending on the electrode configuration, we can deliver unilateral (monaural EVS) or bilateral (binaural EVS) stimulation of the vestibular system. The aim of this research thesis is to investigate vestibular asymmetries in individuals with AIS and matched controls.

Both vestibular perception of rotations evoked by EVS (virtual rotations) and evoked by a rotating motorized chair (real rotations) can be quantified and compared utilizing a psychophysical methodology (Peters et al., 2015). Unilateral vestibular function is compared by taking the absolute difference of the recognition thresholds to monaural EVS. Larger differences in unilateral recognition thresholds will be interpreted as larger vestibular perception asymmetry. I hypothesize that the majority of patients with AIS will exhibit a vestibular asymmetry.

This thesis is structured with a general introduction and literature review, a stand alone paper, and then a general discussion. Chapter 1 of this thesis is a literature review of the relevant research. Chapter 2 is a detailed description of the hypothesis, methodology for this project, results and discussion. Finally, Chapter 3 is a general discussion of the study and future directions for research of vestibular function in individuals with AIS.

Chapter 1: Evidence of vestibular contributions to spinal deformity

Scoliosis

The spine is formed by a series of vertebrae that enclose the spinal cord to protect it. There are five vertebral segments listed in rostral to caudal order: eight cervical, 12 thoracic, five lumbar, five sacral, and one coccygeal vertebrae. Various spinal problems arise when natural anatomical alignment is disturbed, one of these being scoliosis. Scoliosis is a complex three-dimensional spinal deformity, consisting of a lateral deviation and axial rotation of the vertebrae. Idiopathic scoliosis (IS) is a sub-classification of structural scoliosis wherein the vertebral curvature is fixed and cannot be corrected by ipsilateral bending.

Structural scoliosis can be classified in a variety of ways including etiology, age, segments of the vertebral column involved and curve descriptors (Oestreich et al., 1998; Goldstein et al., 1973; Young et al.,1970). If multiple curves are present, the curvature with the largest angle is the primary or major curvature. The direction of scoliotic curvature is based the patient's spinal deviation from the midline from major convex curvature (Goldstein & Waugh, 1973). Most commonly, the major curvature deviates to the right in patients with a thoracic curvature (curvature comprised within the thoracic vertebral region) whereas left major curvatures are relatively rare (Oestreich et al., 1998). For curvatures comprised within both the thoracic and lumbar vertebral region (thoracolumbar curvatures), however, there is no predominant direction (Oestreich et al., 1998). Throughout this thesis, the major convex curvature will be referred to as the "curvature".

The curvature can be assessed utilizing the Cobb method. The Cobb method uses a anteroposterior radiograph to measure the angle of curvature from the vertebral end plates that

have the greatest tilt with respect to the horizontal plane (Cobb, 1948). Intersecting lines from the superior border of the superior vertebra with the greatest tilt and the inferior boarder of the inferior vertebra of the greatest tilt of the curvature segments are drawn. Perpendicular lines from the vertebral lines are drawn and the angle is measured as the angle between these perpendicular lines. Other methods, such as the Scoliometer, provide an estimate of the degree of curvature, but lack information regarding vertebral segments involved (Patias et al., 2010). However, the Scoliometer can be useful to monitor the curvature angle progression (Patias et al., 2010).

Complications of scoliotic curvatures can include: chronic joint pain, decreased respiratory function, cardiac dysfunction, and decreased self-esteem (Angevine et al., 2008; Aulisa et al., 2010; Koumbourlis, 2006). When a Cobb's angle greater than 10^{o} is detected, an individual is considered to have a scoliosis. The greater the curvature, the more interventions may be required such as trunk braces or physical therapy. Curvature angles equal to or greater than 40^{o}, however, are considered a substantial deformity and are more likely to require surgical intervention.

While four of the five types of structural scoliosis have a defined cause (neuromuscular, congenital, developmental, secondary), IS does not. Consequently, its diagnosis is performed by means of elimination. IS scoliosis accounts for approximately 80% of all structural scoliosis cases, and is the type of scoliosis of interest for this research.

Idiopathic Scoliosis

In North America, the prevalence of IS is between 0.47%-5.2% for Cobb's angles less than 40^{o}, with females and males being equally affected (Angevine et al., 2008; Konieczny et al., 2014; Oestreich et al., 1998). The prevalence decreases to between 0.04-0.3% for patients with a

Cobb's angle larger than 40^{o} and females are 10 times more affected than males (Konieczny et al., 2014).

Many factors have been proposed to contribute to IS. These factors include: familial and genetic predisposition, altered control of metabolites and hormones, biomechanical and skeletal muscle abnormalities, and sensorimotor dysfunction. Early work by Sahlstrand et al. (1979) indicated that 40-80% of young patients with scoliosis exhibit "altered equilibrium control" or increased postural sway during balance assessment tasks, suggesting a sensorimotor dysfunction may be a factor in scoliosis. This deficiency in sensorimotor control was confirmed in various balance paradigms altering visual cues and base of support showing that adolescents with IS exhibit increased lateral sway and reactional (hip) strategies to maintain standing posture in comparison to control participants (Haumont et al., 2011; Pialasse et al., 2015; Yamamoto et al., 1982). The implications of these sensorimotor deficits have led to further examination of motor and sensory function in individuals with IS. For example, paraspinal muscular asymmetries have been reported using various techniques including indwelling EMG, muscle biopsy and MRI scans (Ford et al., 1988; Jiang et al., 2017; Mannion et al., 1998; Petersén et al., 1979). Based on MRI scans, the muscular volume on the convex side is larger relative to the concave side, while more fatty infiltration was present on the concave side, alluding to a possible association with muscle atrophy. Furthermore, some authors report increased electromyography (EMG) activity on the convex side; however, it is unclear whether this muscular asymmetry is due to the number of muscle fibers under the electrode, local neurogenic factors or secondary to central nervous system involvement (Cheung et al., 2006; Stetkarova et al., 2016).

Comparatively, proprioception and vestibular function were assessed in individuals with IS to further understand the sensory aspects of their sensorimotor dysfunction. Contradictory

observations on proprioceptive function have been reported in IS patients, showing both asymmetric (Barrack et al., 1984; Wyatt et al., 1986) and symmetric (Byl et al., 1997) perception to vibratory stimulation perception on bilateral sites of the upper and lower extremities. The vestibular system provides cues regarding motion of the head, as well as reflexively adjusts eye movement in regard to the head motion. Probing the vestibulo-ocular reflex (VOR), adolescents with IS show an asymmetrical response to unilateral vestibular stimuli. In addition, IS patients exhibited an increased vestibular-evoked balance response compared to controls to various vestibular stimuli (Pialasse et al., 2015; Sahlstrand et al., 1979a, 1979b; Wiener-Vacher et al., 1998; Yamamoto et al., 1982). These observations suggest that vestibular asymmetry may contribute to spinal deformity. In this thesis, vestibular function will be investigated in individuals with IS. The next sections review briefly the anatomy and physiology the vestibular system as well as methodologies to probe its function in humans.

The vestibular system

The vestibular system contributes to craniocentric self-motion and spatial orientation by encoding for linear and angular accelerations of the head. Consisting of a set of peripheral vestibular end organs in the inner ears, sensory signals from the peripheral vestibular system are sent centrally for processing. The peripheral vestibular system consists of three semicircular canals and two otolith end organs on each side of the head. The semicircular canals are formed from three orthogonal canals (anterior, posterior and horizontal) which encode signals of angular acceleration. The otolith organs consist of the utricles and saccules detecting linear acceleration. These end organs act as mechanotranducers because of the specialized sensory hair cells transduce mechanical signals (accelerations) into electrical signals.

Transduction of signals

There are two types of hair cells within the vestibular end organs, cylindrical Type I and flask-shaped Type II, both containing a kinocilia and a bundle of stereocilia. The afferent fibers discharge spontaneously at rest when no stimulus is applied, either in a regular tonic pattern (regular afferents) or irregular phasic pattern (irregular afferents). Type I hair cells can innervate regular or irregular primary afferent fibers, and Type II hair cells preferentially innervate regular primary afferent fibers (Eatock et al., 2011). The background firing discharge of the afferent fibres (~ 65-90 Hz in squirrel monkey) allows the primary vestibular afferents to encode accelerations bi-directionally (Fernandez et al., 1971). Primary vestibular afferents encode for differing directions by either increasing or decreasing the background firing rate based on the deflection of the stereocilia.

When the head moves, deformation of the hair cells causes a mechanoelectric transduction (MET) (Shotwell et al., 1981). Acting as angular acceleration sensors, the semicircular canals endolymph fluid movement on both sides of the head, can be thought of as a "push-pull" mechanism because of their diametric organization. As the head turns, the endolymph fluid inertia will push the hair cells on ipsilateral side, towards the kinocilia. K^+ channels open and the primary afferent fibres depolarize, opening the voltage-gated Ca^{2+} channel to increase their firing rate. Further, the endolymph fluid on the contralateral side of the head pulls the hair cells away from the kinocilia. The hair cells hyperpolarize causing the K+ channels close and reduces the afferent firing rate.

The otolith organs detect gravito-inertial acceleration acting on the head. Within the otolith is the macula, a sensory region where the hair cells are orientated oppositely on either side of the striola. The otolith organs have an otoconial membrane, a flattened gelatinous

structure with calcium carbonate crystals embedded within. When the head tilts, the otoconial membrane sags and deforms the hair cells in the opposite direction of the head movement. Following the change in firing rate, voltage-gated Ca^{2+} channels and voltage and current-gated K^{+} channels release neurotransmitters, modulating the primary afferent fibre discharge (Lowenstein, 1959).

Neural projections

The sensory signals encoded by the primary vestibular afferents travel along the eight cranial (vestibular) nerve. The primary vestibular afferents project to secondary vestibular neurons. Irregular primary afferents innervate large secondary vestibular neurons and both types of afferents innervate small secondary neurons. Afferents from the eight cranial nerve terminate in the vestibular nuclear complex of the brainstem, the vestibular nuclei (VN), and the cerebellum. The VN is divided into the superior, inferior, medial and lateral VN. The medial VN is mainly innervated by the horizontal semicircular canal, the superior VN is mainly innervated by the anterior and posterior semicircular canal, the lateral VN is mainly innervated by the otoliths organs and posterior semicircular canal, and the interior VN is mainly innervated by the utricle and saccule (Goldberg et al., 1975; Uchino et al., 2005; Zampieri et al., 2014; Sadeghi et al., 2015).

Focusing on VOR, the VN participates in the stabilization of eye movements to maintain a stable visual field. Evidence from alert monkeys indicates that primarily regular vestibular afferents contribute to the VOR (Minor & Goldberg, 1991). The most direct VOR pathway directly synapses from the primary vestibular afferents to neurons in the VN. Within the VN, position-vestibular-pause (PVP) neurons are the primary interneurons which project to the extra-

ocular motor neurons. This short pathway moves the eye 5-6 ms after the head moves (Huterer et al., 2002). PVP neurons are innervated by vestibular inputs but also encode eye position signal and pauses during saccades, a rapid movement of the eye between fixations. A nystagmus is an involuntary eye movement, characterized by a compensatory "slow phase" and a rapid resetting "fast phase" to maintain a stable visual field during head movements (Huterer et al., 2002).

The VN have two functionally distinct descending projections for balance and coordinated head - eye movements: the lateral and medial vestibulospinal tract (Basaldella et al., 2015; Donkelaar et al., 1982; Grillner et al., 1970, 1971). The lateral vestibulospinal tract, which begins at the lateral VN, descends ipsilaterally to all spinal levels. This pathway is crucial for controlling posture and balance, involving the neck, back, hip and leg muscles (Murray et al., 2018). Even though a particular tract may have a unilateral projection, commissural neurons can exert a bilateral influence on proximal and axial muscle control because it synapses on neurons that crosses the spinal cord (Donkelaar et al., 1982). The medial vestibulospinal tract originates primarily in the medial VN and descends bilaterally but only to the cervical and upper thoracic spinal cord. The medial vestibulospinal tract plays a role in controlling head position via axons at the cervical spinal level to control head stabilization (Goldberg et al., 2011). From the VN, secondary vestibular neurons project across the midline and ascend to the thalamus and then project to different cortical regions also carrying information involving the somatosensory, sensorimotor and optokinetic systems. There is no single cortical area designated specifically for vestibular input. Rather, single unit recordings in alert monkeys during physical rotation indicate that vestibular information is largely grouped in the parietal insular vestibular cortex (PIVC), area 3a, and area 7 (Grüsser et al., 1990). A large number of neurons in these areas were vestibularly driven or modulated by vestibular stimuli in macaque monkeys and humans (Garcia

et al., 2018) (Bucher et al., 1998; Suzuki et al., 2001). Other areas of the cortex (i.e. premotor regions of the frontal cortex, parietal areas, and temporal areas) project back to the parietal insular vestibular cortex and brainstem, contributing to balance and stability (Guldin & Grüsser, 1998).

Vestibular signals projecting to the cortex are thought to contribute to conscious perception (Cousins et al., 2013; Pettorossi et al., 2013). Thresholds for the perception of vestibular stimuli involve both regular and irregular afferents in rhesus monkeys but the proportion of the afferents contributing to perception has not been determined (Garcia et al., 2018). In trained monkeys, neuronal and behavioural thresholds were simultaneously measured during rotation discrimination task to assess early sensory processing. A single canal afferent has a threshold that is similar to behavioural thresholds, and there was no significant trial by trial correlation between neuronal activity and perception discrimination (Garcia et al., 2018). In humans, repeated asymmetric whole-body rotations induced progressively more symmetric VOR responses while vestibular perception became progressively more asymmetry, showing differential processing of vestibular information for VOR and perception of motion (Pettorossi et al., 2013).

Methodology: Unilateral and bilateral activation of the vestibular system

Motion stimuli

Rotary and translational head motion induced by voluntary movement, or motorized chairs/platforms can naturally activate the primary vestibular afferent bilaterally. Natural transduction of the peripheral and central vestibular system can be achieved, as described

previously, but always bilaterally. Thus, unilateral vestibular function cannot easily be assessed using real motion stimulation.

Electrical stimuli

Electrical stimuli applied near the vestibular apparatus or over the mastoid processes artificially modulates the vestibular afferent firing rates by stimulating the vestibular nerve and hair cells (Gensberger et al., 2016; Goldberg et al., 1982; Kwan, 2016). When participants are restrained in a chair with their head pitched towards their lap, electrical vestibular stimulation (EVS) evokes a perception of a whole-body raw rotation. Utilizing various electrode configurations, the vestibular system can be stimulated unilaterally or bilaterally (Fitzpatrick & Day, 2004; Goldberg et al., 1982; Kim & Curthoys, 2004). A binaural bipolar electrode configuration (binaural), means that the cathodal electrode is placed over one mastoid while the anodal electrode is positioned over the other mastoid process. A monaural bipolar electrode configuration (monaural) means that one electrode is placed over the mastoid process and the other electrode over C7/T1 vertebrae, forehead or other reference location. Left or right monaural configuration is defined by which mastoid process one of the electrode is placed over. Although often described as unilateral, monaural stimulation is not a pure unilateral stimulation: a 30-45% cross stimulation or "current spread" may be expected due to activation of the contralateral vestibular afferents (Aw et al., 2013).

EVS can be used to elicit a perception of motion, and can be used to quantify vestibular recognition threshold and VOR response (Merfeld, 2011; Peters et al., 2016). Both unilateral and bilateral stimuli provide insight into vestibular function.

EVS perception models

The EVS-induced perception of motion can be manipulated by the head orientation. EVS activates all the vestibular afferents, from both the otoliths and semicircular canals. A model that predicts EVS-induced perception in healthy participants has been formulated and experimentally tested (Day et al., 2004; Day et al., 2005; Della Santina et al., 2005). Mathematically summing the vectors from all vestibular afferents based on the orientation of the end organ they innervate produces a net motion vector. The symmetry of the otolith end organ vectors, however, cancel each other (Mian et al., 2010). The resulting net motion is a rotation vector pointing posteriorly and 18.8^{o} above Reid's plane (a plane passing through the inferior margin of the infra-orbital rim and through the center of each bony external auditory meatus bilaterally) (Day et al., 2005; Della Santina et al., 2005; Mian et al., 2010). Pitching the head forward (so that Reid's plane is 18.8^{o} from vertical) aligns the net EVS-induced motion vector with Earth's vertical axis. This allows participants to perceive a whole-body yaw rotation that is indiscernible from a real yaw rotation (Figure 1).

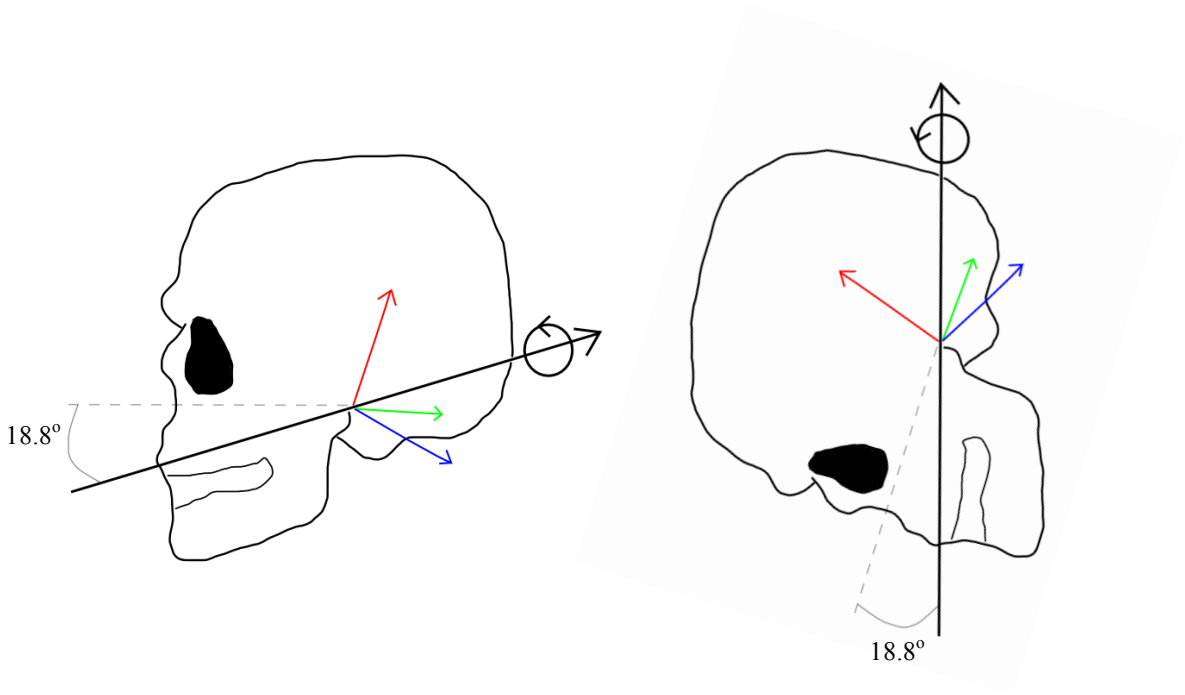

Figure 1. EVS net vector and head orientation

The net EVS vector based the activation of all vestibular afferents (the otolith end organs cancel each other bilaterally). When Reid's plane is 18.8° from Earth's vertical axis, the net vector from the semicircular canal can be aligned with Earth's vertical axis (Right). (Blue arrow = horizontal semicircular canal vector. Red arrow = anterior semicircular canal vector. Green arrow = posterior semicircular canal vector. Black arrow = the net vector summed from all six semicircular canals. Dotted grey line = Reid's plane.)

Vestibular asymmetry in Adolescent Idiopathic Scoliosis

Various studies in animals and humans point to vestibular asymmetry in adolescents with IS. Frogs represent an advantageous model because young frogs have limited limb usage, similar to human newborns. Unilateral labyrinthectomy during stages 50-60 days of development (larval phase) caused a deformation of the spine, similar to the spinal deformity of scoliosis in humans (Lambert et al., 2009). The spinal deformity continued to develop into frogs' young adult phases and persisted during adult phase, further resembling scoliosis in humans. In humans, asymmetric semicircular canal orientation has been quantified in individuals with IS. Two research groups have reported the asymmetric horizontal semicircular canal orientation in participants with IS (Hitier et al., 2015; Shi et al., 2011). Caloric vestibular stimulation in individuals with IS indicated that IS participants had an 8.6% asymmetric gain in VOR response in comparison to controls that showed a 3.7% vestibular asymmetry (Sahlstrand et al., 1979a). These observations, however, were not replicated in more recent work (Hitier et al. 2015).

Aim of the thesis

The aim of this thesis was to investigate vestibular function in individuals with AIS. Utilizing monaural EVS, we aimed to quantify vestibular asymmetries in individuals with AIS in comparison to controls by assessing their perception of virtual yaw rotations to unilateral vestibular stimuli. We hypothesize that individuals with AIS will exhibit an asymmetric perception of unilateral vestibular stimuli. This thesis research will provide information about the asymmetric vestibular function of individuals with AIS.

Chapter 2: Experiment – Vestibular perception evaluation

Introduction

Adolescent idiopathic scoliosis (AIS) is the most prevalent type of idiopathic scoliosis. AIS is differentiated from other idiopathic scoliosis by the onset of scoliotic curvature development occurring between 10 -16 years old (Manzoni & Miele, 2002). Although the exact cause of AIS remains unknown, multiple factors, including a sensorimotor dysfunction, have been proposed (Machida, 1999; Wang et al., 2011). Specifically, asymmetric vestibular function resulting in imbalanced descending drive to the spinal musculature has been implicated as a potential factor contributing to the development of scoliosis (Hawasli et al., 2015; Lambert et al., 2009; Sahlstrand et al., 1979a, 1979b). The most compelling evidence that vestibular asymmetry may result in scoliosis stems from work in tadpoles. Unilateral removal of the tadpole vestibular labyrinth during its larval phase resulted in a spinal curvature similar to scoliosis that persisted into adulthood (Lambert et al. 2009). In humans, Shi et al. (2011) reported asymmetric semicircular canal orientation in females with a right thoracic scoliotic curvature, a finding corroborated by Hitier et al. (2015). Individuals with AIS also exhibit asymmetric vestibular function (VOR and vestibular-evoked balance responses) to caloric vestibular stimuli in comparison to control participants (Sahlstrand et al., 1979a, 1979b) but these results require further investigation (Hitier et al., 2015). Caloric vestibular stimuli, however, may not be the best tool to evaluate vestibular function in young individuals due to the induced vertigo and nausea.

An alternative method to assess asymmetric vestibular function is electrical vestibular stimulation (EVS) applied over the mastoid processes (Day & Fitzpatrick, 2005; Fitzpatrick & Day, 2004). EVS activates all semi-circular canal and otolith primary vestibular afferents, the

cathodal current increases the firing rate of the afferents, and anodal current decreases the firing rate (Goldberg et al., 1984; Kim & Curthoys, 2004). EVS induces a net equivalent motion vector (EVS vector) based on the vectorial summation of peripheral vestibular components (Day & Fitzpatrick, 2005; Fitzpatrick & Day, 2004). According to this model, EVS applied bilaterally over the mastoid processes (i.e. in a binaural bipolar configuration) results in a net rotation around a vector pointing posteriorly and 18.8^{o} above Reid's plane (Day & Fitzpatrick, 2005; Fitzpatrick & Day, 2004; Mian et al., 2010). Hence, when seated participants pitch their head down to align the EVS vector with Earth's vertical, binaural bipolar EVS induces a perception of yaw rotation (virtual rotation about the vertical axis) that is indistinguishable from a real rotation (Day & Fitzpatrick 2005; Peters et al., 2016). When the electrodes are applied over a mastoid process and C7-T1 (i.e. monaural configuration), EVS preferentially activates the primary vestibular afferents ipsilateral to the stimulated mastoid process, permitting the assessment of vestibular asymmetry (Aw et al., 2013). Using monaural and binaural EVS configurations, vestibular function and asymmetry can be characterized using vestibular recognition thresholds (Karmali et al., 2016; Merfeld, 2011).

The aim of this study was to investigate vestibular function and asymmetry in individuals with AIS and age-, and sex-matched control participants. Vestibular perception thresholds of virtual (EVS) rotations and real (chair) rotations were quantified using a forced-choice recognition task (Peters et al., 2015). Asymmetric vestibular function was estimated by computing the absolute difference of the recognition thresholds between the left and right monaural EVS conditions. We hypothesized that participants with AIS would exhibit an asymmetric vestibular response to unilateral vestibular stimuli. Further, we wanted to quantify the unilateral vestibular dysfunction in comparison to controls, to further characterize the

asymmetry. Finally, given the asymmetric semicircular canal orientation previously reported in individuals with AIS (Shi et al., 2011), we modelled the effect of this asymmetry on the net vector induced by monaural and binaural EVS. This model enabled us to establish if the asymmetric vestibular function observed in individuals with AIS was related to a structural asymmetry in their semicircular canals

Methods

Participants

Ten healthy participants with AIS between the ages of 12 and 16 years old (8 females, 2 males), and ten healthy age- and sex-matched control participants (8 females, 2 males) with no known history of ontological or neurological disorder participated in this study (Tables 1 and 2). AIS participant's Cobb's angles were recorded from their clinical chart, measured from an anteroom-posterior radiograph by an orthopaedic surgeon. All measurements were taken within three months of the experimental testing except for the pre-surgical measurements that was measured three and seven months prior to testing. Although a definitive diagnosis cannot be made without measuring the Cobb angle on a radiograph, control participants were screened for scoliosis using the Adam's Forward Bend Test. Trunk rotation angle was measured using an application (Scoliometer, Health in Your Hands, Singapore) on a smartphone (iPhone 6S, Apple Inc, Cupertino, CA, USA) at three locations: upper thoracic (T3/T4 vertebrae); main thoracic (T6-T9 vertebrae); and thoracolumbar (T12/L1 vertebrae) (Patias et al., 2010; Prowse et al., 2016). Any control participant with a trunk rotation angle above 5^{o} was excluded.

The experimental protocol was explained to each participant and their legal guardian. Written and informed assent and consent were obtained from the participant and legal guardian, respectively. All procedures conformed to the Declaration of Helsinki and were approved by the clinical research ethics board of the University of British Columbia.

Table 1. Experimental group characteristic comparison

	Participants with AIS mean (SD)	**Control Participants** mean (SD)	**p value**
Age (year)	14.1 (1.5)	14.1 (1.7)	p = 1.00
Height (cm)	162.1 (6.2)	163.0 (9.1)	p = 0.79
Weight (kg)	52.1 (8.6)	49.1 (7.0)	p = 0.39

Table 2. AIS participant's descriptive characteristics of major curvature

Sex	**Surgery prior to testing**	**Cobb Angle**	**Location**	**Direction**
F	No	26°	T5-T11	Right
F	No	29°	T5-T11	Right
F	No	32 °	T5-T11	Right
F	No	34°	T5-T11	Right
F	No	35 °	T5-T11	Right
F	No	37°	T8-L2*	Left
F	No	42°	T10-L3*	Left
F	Yes	61°**	T9-L3*	Left
M	No	66°	T6-T12	Right
M	Yes	79°**	T5-T12	Right

M = male; F = female.
Cobb angle measurements were obtained from anterio-posterior radiographs. Direction indicates the direction of deviation from the mid-sagittal plane of the major convex curvature.

** Thoracolumbar curvature*
*** Pre-operative curvature measurement*

Electrical vestibular stimulation

EVS was delivered using two different electrode configurations: monaural bipolar for unilateral activation of the vestibular afferents, or binaural bipolar for bilateral activation of the vestibular afferents. The monaural bipolar electrode configuration consisted of one carbon rubber electrode (9 cm^2) placed over the mastoid process and the other electrode over the C7/T1 vertebrae (Figure 2). Each electrode was secured with surgical tape. Left and right monaural bipolar configurations refer to the electrode being positioned on the participant's left and right mastoid process, respectively. For the binaural bipolar electrode configuration, the electrodes were also positioned on mastoid processes and C7/T1 vertebrae, with two independent stimulus isolation units controlling the stimuli (Figure 2). This dual-stimulus approach was preferred over using a single stimulus isolation unit to exclude the possibility of an unforeseen stimulus interaction associated with a change in the current paths between electrode configurations (Day et al., 2010). Each electrode and electrode location were cleaned with alcohol and each electrode was coated with 1 cm^3 of conductive electrode gel (Spectra 360, Parker Laboratories, Inc., Fairfield, NJ, USA) to maintain similar electrode impedance (~5 kOhms), as measured by an impedance meter (F-EZM5, Astro-Med Inc. (now AstroNova), West Warwich, RI, USA).

The electrical vestibular stimuli were generated on a PC computer with custom LabVIEW software (v2013, National Instruments, Austin, TX, USA) and sent directly to either one, or both, constant-current isolation units (STMISOL, Biopac System, Goleta, CA, USA) via a multifunction data acquisition board (PXI-6289, National Instruments, Austin, TX, USA). Current and voltage monitoring cables (STM100C and STM100V, Biopac Systems, Goleta, CA, USA) measured the current and voltage applied to the participants. These signals were digitized at a sampling frequency of 100 Hz (PXI-6289, National Instruments, Austin, TX, USA) and

stored on a local computer. In addition, the electrode impedance was compared between the left and right monaural configurations as well as between groups to ensure the impedance level were equal.

In order to minimize non-vestibular cues associated with the electrical stimuli, the skin under the electrodes was anesthetized with AMETOP (tetracaine HCl gel 4%, Smith & Nephew Medical Ltd., Hull, UK) applied approximately 30 minutes prior to the electrode placements. In addition, each participant wore a blindfold, earplugs, noise-cancelling headphones (Quiet Comfort 25, Bose, Framingham, MA, USA) and memory foam padding surrounding the trunk to further minimize other sensory cues.

Real rotations

Real rotations stimulate the primary vestibular afferents bilaterally to elicit sensations of rotation. Rotation stimuli were delivered using a custom-built rotary chair (Figure 2). Participants were physically rotated using a servo-controlled AC motor (SGM7D-2ZN, Yaskawa, Japan; angular resolution 0.00034^{o}). A motion controller (PXI-7350 and UMI-7774, National Instruments, Austin, TX, USA) sent torque commands to a servo amplifier (SGDV-200A01A, Yaskawa, Japan) to generate motion profiles programmed via custom-built LabVIEW software with the NI motion-programming suite (v2013, National Instruments, Austin, TX, USA).

Participants were seated atop the motor on a chair, in the same head orientation as the EVS conditions. This head orientation does not change participant's perception sensitivity to real yaw rotations (Peters et al., 2015). In addition, each participant wore a blindfold, earplugs, noise-cancelling headphones (Quiet Comfort 25, Bose, Framingham, MA, USA) and memory foam padding surrounding the trunk to further minimize other sensory cues, as described above.

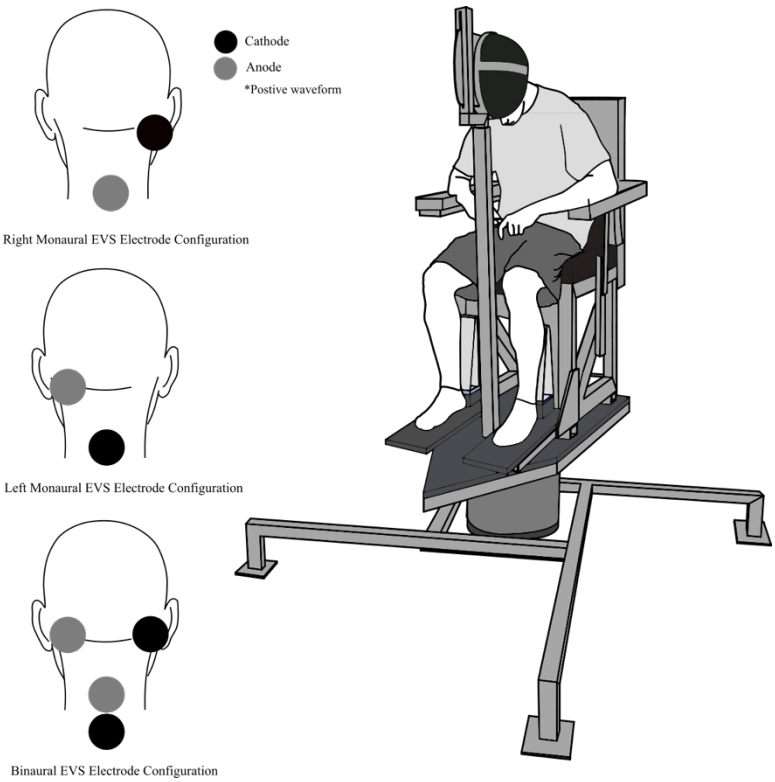

Figure 2. Experimental set up for virtual and real rotations.
Left. Electrode configurations for EVS stimulation to induce virtual rotations. Electrode polarity is indicated for a positive waveform. Right. Rotary chair and helmet set up to ensure proper head orientation.

Vector summation model

Binaural bipolar EVS: Summing the vector from each semicircular canal on one side results in a rotation vector that is pointing backwards with a small upwards (~18^{o}) and lateral component (~3^{o}). The other side would be the same except for an inverted lateral component, because of the polarity of the current. The otolith components cancel bilaterally (Mian et al., 2010). Summing all the semicircular canal orientation vectors indicates that the binaural bipolar EVS net virtual rotation is around a vector pointing posteriorly in the head, at 18.8^{o} above Reid's plane (Day, Elijane, Welgampola, & Fitzpatrick, 2011; Fitzpatrick & Day, 2004) (Equation 1), where R denotes the resultant vector and LA, LH, LP, RA, RH, RP denote the vectors from the anterior, horizontal, and posterior semicircular canal on the left and right side respectively (Table 3).

Equation 1. Summed vector equation for binaural bipolar EVS

$$R_{binaural} = (LA+LH+LP+RA+RH+RP)$$

Pitching the head forward by 71.2^{o}, the net EVS vector can be aligned with the Earth's vertical axis (Fitzpatrick & Day, 2004), inducing a perception of whole-body yaw rotation that is indistinguishable from the perception of real yaw rotations elicited by a chair rotation (Day & Fitzpatrick, 2005; Fitzpatrick & Watson, 2015; Peters et al., 2015; St. George & Fitzpatrick, 2011; Wardman et al., 2003).

Monaural bipolar EVS: Using the same summed vector operations approach described above for binaural bipolar EVS, the net motion induced by monaural EVS can be estimated. Based on balance responses to binaural and monaural EVS, the prediction of otolith response did

not match the balance response (Mian et al., 2010). While the otolith afferents are stimulated by EVS, the effect of the otolith net vector must be very small and we assumed it did not affect the net rotation vector. Assuming all semicircular canal afferents respond EVS, a net virtual rotation around a vector that is pointing posteriorly, 18.8^{o} above Reid's plane and about 3^{o} laterally from the midline is expected (Equation 2).

Equation 2. Summed vector equation for monaural bipolar EVS

$$R_{left\_monaural} = (LA+LH+LP)$$
$$R_{right\_monaural} = (RA+RH+RP)$$

During monaural bipolar EVS, however, some cross stimulation may activate the vestibular primary afferents from the opposite labyrinth (i.e. contralateral to the mastoid electrode). Aw et al. (2013) reported that monaural unipolar EVS applied to the deafferented side in a patient with a unilateral vestibular system evoked ocular responses about one-third the size of those evoked by binaural bipolar EVS. Using the summed vector operations model, we explored the amount of expected cross stimulation during monaural EVS in control participants. Briefly, assuming no cross stimulation between sides during monaural EVS, we expected the recognition thresholds to monaural EVS to be twice those expected during binaural EVS. Any deviation from this prediction was examined by adjusting the predicted level of cross stimulation during monaural EVS until the ratio of the observed binaural/monaural EVS threshold could be explained. We adjusted the level of cross stimulation from -100% to 100% in 10% steps (negative values are current spreading from the mastoid electrode and positive values are current spreading from the C7/T1 electrode with the current spreading to the opposite primary afferents).

Equation 3. Summed vector equation for monaural bipolar EVS with current spread

$$R_{right\_monaural} = (\%\ cross\ stimulation)(LA+LH+LP)+ (RA+RH+RP)$$
$$R_{left\_monural} = (LA+LH+LP) + (\%\ cross\ stimulation)(RA+RH+RP)$$

To determine if structural asymmetry in semi-circular canals reported by Shi et al. (2011) affected the functional asymmetry observed in individuals with AIS, we modeled the altered angle between the left anterior and horizontal semicircular canals compared to the right-side counterparts (Table 4). First, we estimated the vector component pointing along Earth's vertical for all EVS configurations and normalized all vectors by the recognition thresholds to binaural bipolar EVS observed in participants with AIS. We simulated rotations between the anterior and horizontal semicircular canals from -12^o to 12^o, in directions further or closer towards the anterior canal (in 3^o steps). For completeness, we computed the predicted effects of structural changes in semi-circular canal orientations for cross stimulation ranging from -100% to 100% (in 10% steps) (negative values are current spreading from the mastoid electrode and positive values are current spreading from the C7/T1 electrode with the current spreading to the opposite primary afferents). LH_{AIS} denotes the changed left horizontal semicircular canal orientation of individuals with AIS.

Equation 4. Summed vector equation for monaural bipolar EVS with current spread based on AIS patient's semicircular canal orientation.

$$R_{right\_monaural} = (\%\ cross\ stimulation)(LA+LH_{AIS}+LP) + (RA+RH+RP)$$
$$R_{left\_monural} = (LA+LH_{AIS}+LP) + (\%\ cross\ stimulation)(RA+RH+RP)$$

Table 3. Semicircular canal plane unit normal vector coefficients from Della Santina et al., 2005

	LA	LH	LP	RA	RH	RP
X	-0.5893	-0.3227	-0.6943	-0.5893	-0.3227	-0.6943
Y	0.7884	-0.0384	-0.6669	-0.7884	0.0384	0.6669
Z	-0.1766	0.9457	-0.1766	-0.1766	0.9457	-0.1766

L = left, R = right; A, H, P = anterior, horizontal and posterior semicircular canal, respectively. (X, Y, Z) = Cartesian position defined in the Reid stereotaxic system.

Table 4. Semicircular canal plane unit normal vector coefficients calculated from Shi et al.'s results (2011)

	Modelled AIS Left Horizontal Semicircular Canal Orientation (LH_{AIS})								
	-12 °	**-9 °**	**-6 °**	**-3 °**	**0 °**	**3 °**	**6 °**	**9 °**	**12 °**
X	-0.4692	-0.4342	-0.3981	-0.3609	-0.3227	-0.2836	-0.2437	-0.2031	-0.1619
Y	-0.1654	-0.1341	-0.1022	-0.0705	-0.0384	-0.0062	0.0260	0.0581	0.0901
Z	0.8675	0.8908	0.9116	0.9299	0.9457	0.9695	0.9695	0.9774	0.9827

(X, Y, Z) = Cartesian position defined in the Reid stereotaxic system. 3^o was the orientation reported by Shi et al., however, the rotation directions were expanded to determine if other rotations could explain any asymmetry from this experiment.

Vestibular recognition threshold estimation

Participants were asked to discern whether the direction of the virtual or real rotations was to the right or left (forced-choice task). Participants were seated atop the rotary chair with their head pitched down towards their lap and held securely with a helmet braced to the rotary chair carriage. The experimenter confirmed that the head was pitched downwards ~71^{o}, aligning the angle of the EVS-evoked rotational vector with an Earth-vertical axis and the external acoustic meatus is over the axis of chair rotation (Fitzpatrick & Day, 2004). Correct head orientation was confirmed by the experimenter with a protractor numerous times during testing.

Participants completed the real rotations first, in order for the AMETOP cream to properly anesthetize the skin, then the virtual rotation electrode configuration was randomized for each participant. Participants completed a series of 50 trials for each condition. For all trials, they were exposed to a single cycle raised-cosine EVS (direct current: mA) or real velocity pulse (angular velocity: ^{o}/s) at 0.1 Hz (Figure 3A). Participants were required to indicate which direction they were rotated with a verbal response ("left" or "right"). The electrode polarity and rotation direction were randomized across trials. Feedback was given about the correctness of the response. Participants were also informed when the subsequent stimulus would be delivered. During EVS, participants reported vivid sensations of being rotated in the chair even though the chair remained stationary. The correct direction of virtual rotation was always toward the cathode side.

The peak amplitude of the stimuli was varied across trials using a Bayesian adaptive procedure (Kontsevich & Tyler, 1999; Peters et al., 2015). From each participant's performance, a psychometric function relating the amplitude of the vestibular stimulus (in ^{o}/s or mA) to the proportion of correct direction recognition was fitted (Figure 3B). A sigmoidal psychometric

function for each participant was parameterized as a modified Weibull function (Tong, et al., 2013) (Equation 5) (Figure 3C).

Equation 5. Modified Weibull function.

$$P(\text{correct}|x) = \gamma + (1 - \gamma - \delta)(1 - 2^{-(x/a)^b})$$

The γ parameter sets the y-intercept of the psychometric curve, the *a* parameter determines the lateral position of the psychometric curve along the *x*-axis, the *b* parameter determines the slope of the psychometric curve, and the δ parameter represents the lapse rate. A lapse rate was included to account for the realistic possibility of occasional attention lapses, resulting in 50% correct response probability regardless of the stimulus amplitude (Peters et al., 2015). The γ parameter was set at 0.5 in this experiment because of the chance performance that could happen in a forced-choice task.

For the virtual rotations (EVS trials), the current stimulation amplitude could reach a peak of 5 mA and was adjusted in steps of 0.08 mA. For the real rotations, the chair rotated up to 10 ^{o}/s and was adjusted in steps of 0.25 ^{o}/s. For both virtual and real rotations, participants received five practice trials at 2 mA and 5 ^{o}/s, respectively. All participants could perceive the direction of rotation in 100% of the practice trials, ensuring they could complete the task.

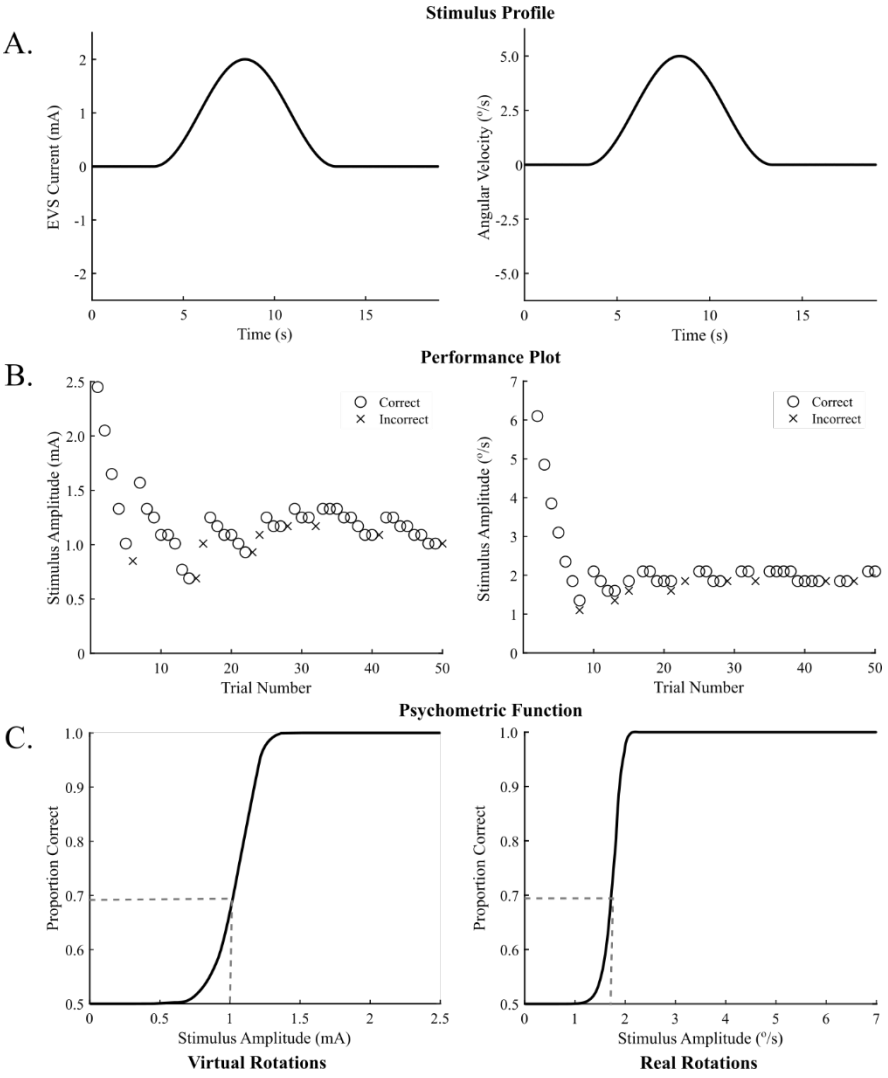

Figure 3. Experimental set-up.

A. Stimulus profile, single cycle raised cosine curve at 0.1Hz. B. Exemplar performance plot, correct responses denoted by o's and incorrect responses denoted in x's. C. Exemplar psychometric function fitted from the performance plot (B.). 69% proportion correction is the recognition threshold (dotted line).

Statistical analysis

The recognition threshold value was defined as the peak stimulus level at which the participant could correctly discriminate rotation direction with 69% probability (real rotations: ^{o}/s; virtual EVS rotations: mA), which corresponds to a discriminability index (d') equal to 1 for this one-interval direction recognition task (Gescheider, 1997). In this experiment, the d' referred to the theoretical separation between response distributions for right and left rotations, normalized by the standard deviation which was assumed to be equal for both directions (Peters et al., 2015).

Nonparametric or parametric tests were applied to the data based on the results of the normality of the data (Shapiro-Wilk test) as well as the equality of the variance between the two groups (Levene's test). If the data were found to be non-normally distributed and unequal variance, the non-parametric tests, Mann-Whitney U tests and Rank-Biserial Correlations were performed. If the data were found to be normally distributed and equal variance, the parametric tests, Student's t-tests and Cohen's d tests were used.

All statistical analyses were performed with JASP (v0.8.6, The JASP Team, The Netherlands). Results from parametric analyses were reported as mean (standard deviation (SD)) and those from non-parametric analyses as median (1^{st} quartile, 3^{rd} quartile) (Drummond & Tom, 2012). Statistical significance was set at alpha (α) < 0.05.

Unilateral vestibular stimuli

To assess vestibular perception asymmetry, we calculated the absolute difference between each participant's monaural recognition thresholds (mA). Mann-Whitney U tests were used to compare the vestibular asymmetry (mA) between experimental groups. The effect size

was evaluated with a Rank-Biserial Correlation. To determine whether vestibular asymmetry was associated with an unusually high or low recognition thresholds to unilateral stimuli, we categorized each participant's left and right monaural recognition thresholds as either "high" or "low" based on which of these two values was higher or lower relative to each other. Then these "high" and "low" thresholds were compared between groups utilizing Mann-Whitney U tests.

A Pearson's correlation was used to characterize the relationship between the monaural recognition threshold magnitude (mA) and the Cobb's angle (^{o}) of the curvature. The monaural recognition threshold magnitude of each AIS participant was calculated, subtracting their right monaural recognition threshold by their left monaural recognition threshold (mA). A right-biased vestibular asymmetry was indicated by a positive value, and a left-biased vestibular asymmetry was indicated by a negative value. The Cobb's angle of each AIS participant was obtained from radiologists' reports. Right Cobb's angles (direction of deviation from the midline of the major convex curvature) were represented with positive values and left Cobb's angles with negative values. For further exploration, additional correlations were completed either excluding the AIS participants with spinal fusion surgery and using the post-operative Cobb's angle of AIS participant with spinal fusion surgery.

Bilateral vestibular stimuli

Vestibular recognition thresholds of bilateral stimuli (virtual rotations to binaural bipolar EVS and real rotations) were compared using Student's t-tests.

Model simulation

To assess if the vestibular perception asymmetry could be explained by asymmetric vestibular system orientation, a single sample t-test was used to compare the modelled effect of AIS vestibular asymmetry based on the modelled recognition threshold to monaural EVS and the recognition threshold in the results.

Results

Vestibular asymmetry: Recognition threshold to unilateral activation

To determine if participants with AIS exhibited asymmetric recognition threshold to vestibular stimuli, we used monaural bipolar EVS. The absolute difference of monaural recognition thresholds was larger in participants with AIS than control participants (Figure 4). The monaural recognition threshold differences ranged from 0.22 - 1.00 mA for participants with AIS and 0.01 - 0.21 mA for control participants. These observed differences were confirmed by the Mann-Whitney U tests ($W = 100.00$, $p < 0.001$, Rank-Biserial Correlation = 1.00), with median recognition threshold differences of 0.53 (0.37, 1.00) mA for participants with AIS and 0.06 (0.05, 0.21) mA for control participants.

Categorizing each participant's monaural recognition threshold (left or right) into "high" and "low" revealed that the "high" monaural recognition threshold of participants with AIS was significantly larger than the control participant "high" monaural recognition threshold (Figure 5). The median monaural "high" recognition thresholds for individuals with AIS was 1.67 (1.61, 3.25) mA compared to 1.35 (1.17, 1.91) mA for control participants ($W = 88.00$, $p = 0.003$, Rank-Biserial Correlation = 0.76). In contrast, the "low" monaural recognition threshold of

participants with AIS was similar to that of control participants (1.16 [1.04, 2.25] vs 1.26 [1.15, 1.71] mA; W = 51.00, p = 0.97, Rank-Biserial Correlation = 0.02).

To determine if there was a relationship between the participants with AIS spinal curvature (pre-operative Cobb's angle for participants with spinal fusion surgery) and their monaural threshold differences, we performed a correlation analysis and no relationship was observed (r = -0.37, r^2 = 0.14, p = 0.30) (Figure 6A). Further explorations of this relationship were performed. Both excluding the participants with spinal fusion surgery and including the post-operative Cobb's angle for AIS participants with spinal fusion surgery yielded a significant negative relationship between spinal curvature and monaural recognition threshold difference (r = -0.69, r^2 =0.48, p = 0.03 and r = -0.823, r^2 =0.68, p = 0.01, respectively) (Figure 6B and 6C).

Recognition thresholds to bilateral vestibular activation

To measure the recognition thresholds of bilateral vestibular activation, real rotations and binaural bipolar EVS were used. The real rotation recognition thresholds ranged from 1.6 – 3.2 ^{o}/s for participants with AIS and 1.4 – 2.7 ^{o}/s for control participants. The mean recognition threshold for participants with AIS was 2.2 (0.5) ^{o}/s and for control participants was 2.0 (0.5) ^{o}/s, and they were not statistically different from each other (t_{18} = 0.64, p = 0.53, d = 0.53) (Figure 7). The recognition thresholds to binaural bipolar EVS ranged from 0.59 – 1.82 mA for participants with AIS and 0.18 – 1.15 mA for control participants. The mean recognition thresholds were 1.15 (0.43) and 0.89 (0.31) mA for AIS and control participants, respectively (t_{18}= 1.54, p = 0.14, d = 0.69) (Figure 7).

Modeling the effects of structural vestibular asymmetry on vestibular perception in individuals with AIS

In control participants, the recognition thresholds of binaural bipolar EVS was 70% of those observed in response to monaural EVS (0.89 mA vs. 1.24 mA). These observations deviate from the prediction assuming no cross stimulation during monaural EVS (50%; see Figure 8). Adjusting the predicted cross stimulation during monaural EVS, our model indicated that 40% of the current during monaural EVS from the C7/T1 electrode stimulates the opposite vestibular primary afferents. Assuming 40% cross stimulation, the monaural EVS-evoked net rotation vector remains 18.8^{o} above Reid's plane but deviates only 1.3^{o} from the midline (towards the stimulated ear; Figure 8). Using the 40% cross stimulation during monaural EVS, we explored the effects of the angle between the left anterior and horizontal semicircular canals reported in individuals with AIS on the asymmetry in vestibular function observed here (Figure 8).

We calculated the absolute difference between the predicted left and right normalized monaural EVS vectors when altering the angle between the left anterior and horizontal semicircular canals. When the angle between the left anterior and horizontal semicircular canals was 3° smaller than their right-side counterparts, the predicted absolute difference in recognition threshold was 0.007 mA. This difference was smaller than the mean monaural recognition threshold difference observed in individuals with AIS (0.53 (0.37, 1.00) mA vs. 0.007 mA, t_8 = 10.05, $p < 0.001$). We further explored larger semicircular canal orientation and cross stimulation revealing that the largest predicted absolute difference in recognition threshold was 0.1 mA (at 12^{o} structural asymmetry and 100% cross stimulation; 0.53 (0.37, 1.00) mA vs. 0.1mA, t_8 = 8.638, $p < 0.001$; Figure 9). Based on our simulations, functional vestibular asymmetry reported cannot be explained by asymmetry in semicircular canal orientation alone.

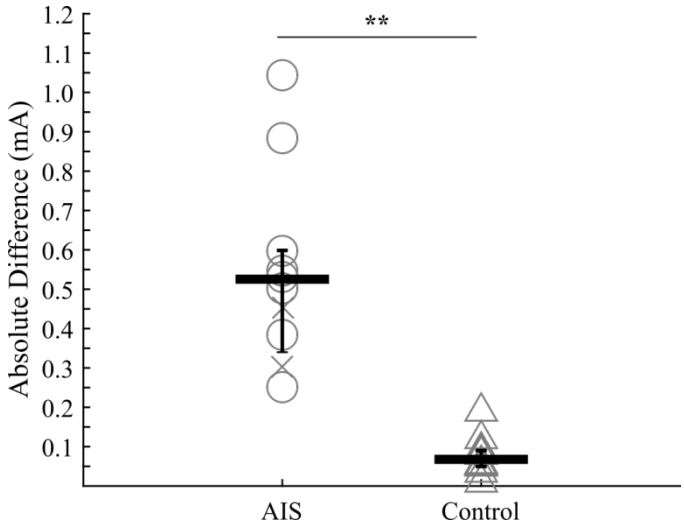

Figure 4. Unilateral vestibular stimuli results.
*The absolute difference of each participant's monaural EVS recognition threshold (**p < 0.001).*
(Circle = AIS participant, X = AIS participant with spinal fusion surgery; Triangle = Control participant; Bold line = median; Error bars = IQR).

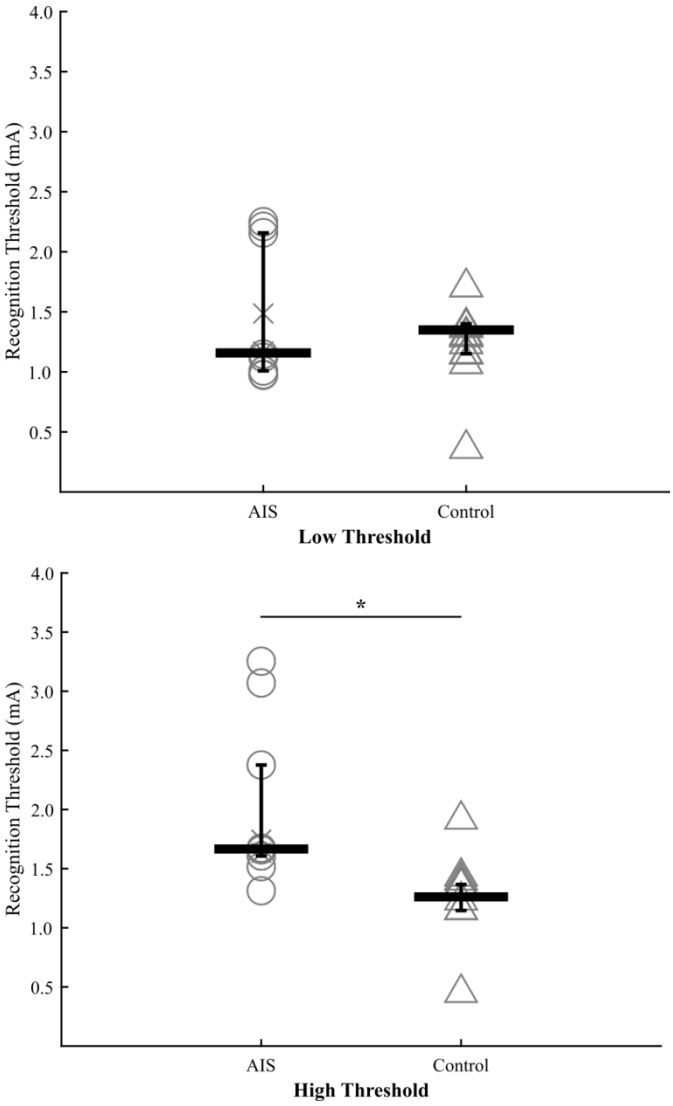

Figure 5. Low and high monaural EVS recognition threshold comparison.
Top. The "low" monaural recognition threshold of each participant ($p > 0.05$). Bottom. The "high" monaural recognition threshold of each participant ($p < 0.01$).*
(Circle = AIS participant; X = AIS participant with spinal fusion surgery; Triangle = Control participant; Bold line = median; Error bars = IQR).

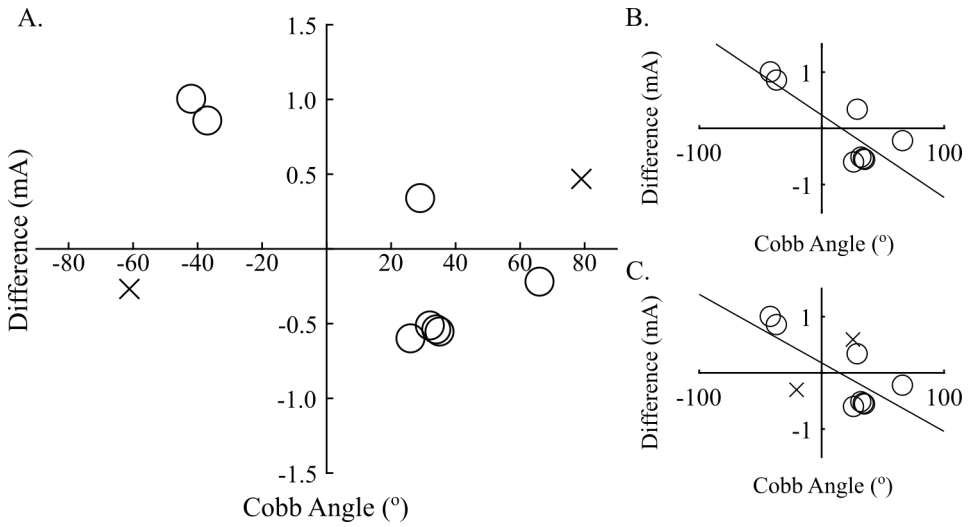

Figure 6. The correlations of AIS participant's Cobb's angle and vestibular perception asymmetry.

A right curvature was indicated by a positive value, and a vestibular asymmetry with higher right threshold was indicated by a positive value, located in the top right corner. A left curvature was indicted by a negative value and a vestibular asymmetry with a higher left threshold was indicated by a negative value, located in the bottom left corner.

A. Correlation of AIS participant's Cobb's angle (spinal fusion participant's pre-operative Cobb's angle (n =2)) and monaural recognition threshold difference (r = -0.37, r^2 = 0.14, p = 0.30).

B. Correlation of AIS participants Cobb's angle (excluding participants with spinal fusion surgery) and monaural recognition threshold difference (r = -0.823, r^2 =0.68, p = 0.01).

C. Correlation of AIS participants Cobb's angle (spinal fusion participant's post-operative Cobb's angle (n=2)) and monaural recognition threshold difference (r = -0.69, r^2 =0.48, p = 0.03).

(Circle = individual AIS participant, X = AIS participant with spinal fusion surgery).

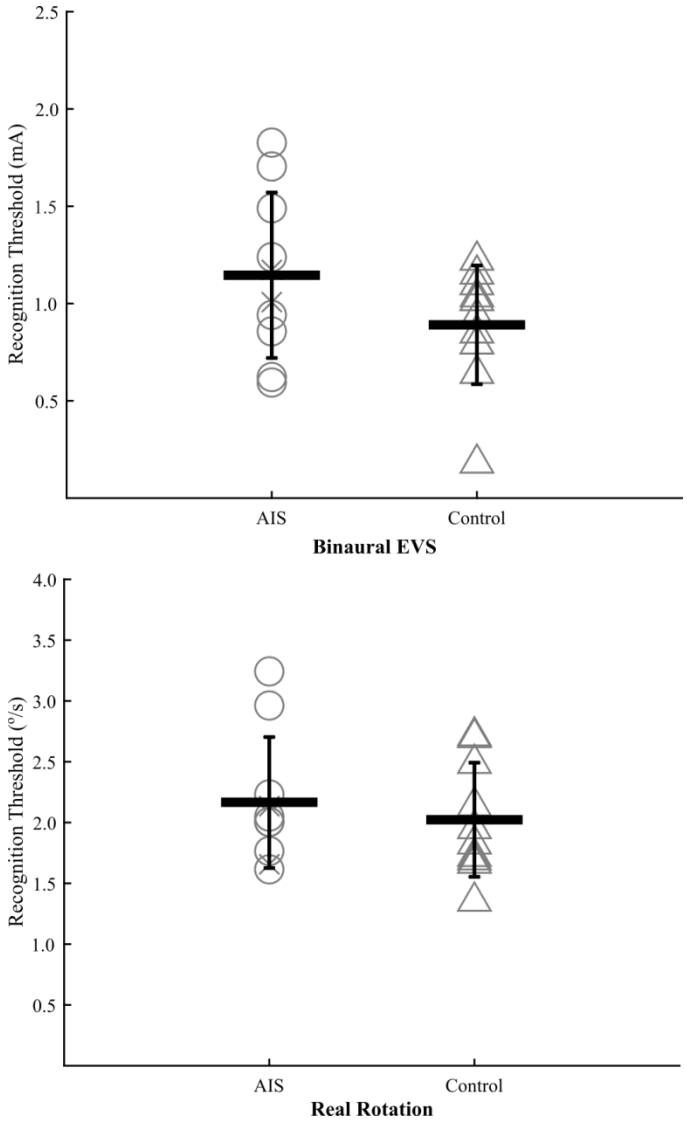

Figure 7. Bilateral vestibular stimuli results.
Top. The binaural recognition thresholds (p>0.05). Bottom. The real rotation recognition thresholds (p>0.05).
(Circle = AIS participant; X =AIS participant with spinal fusion surgery; Triangle = Control participant; Bold line = mean; Error bars = SD).

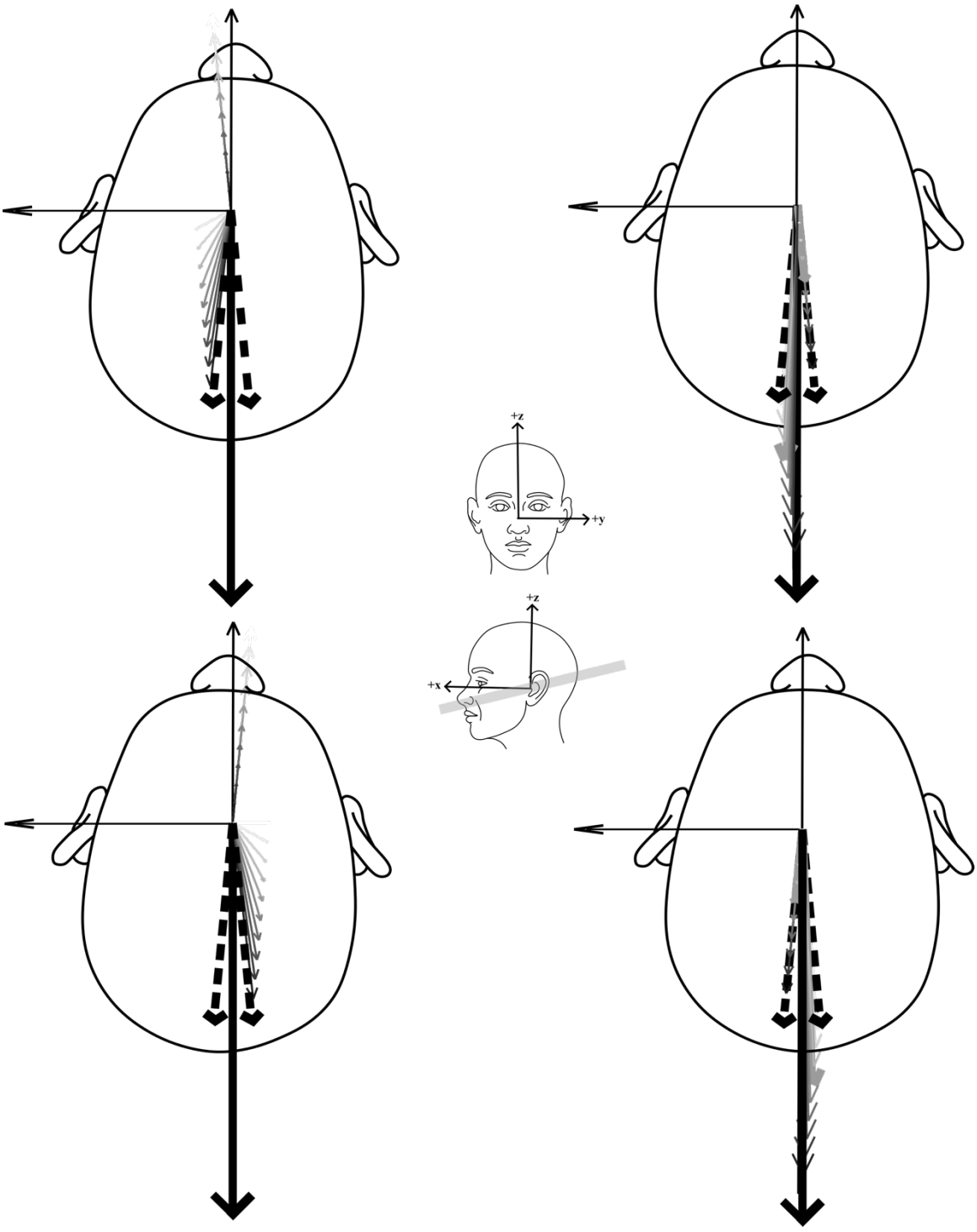

Figure 8. Simulated current spread.
The current spread vector and net monaural vector accounting for the current spread. Each grey arrow is a 10% step in current spread.
Top left: Left monaural EVS with current spread from the mastoid electrode. Top right: Left monaural EVS with current spread from the C7/T1 electrode. Bottom left: Right monaural EVS

with current spread from the mastoid electrode. Bottom right: Right monaural EVS with current spread from the C7/T1 electrode. Faces in the middle are the reference frame, the plane view of each face is the grey bar in the reference frame. (Black thick arrow = binaural bipolar net vector, Dashed thick arrow = monaural bipolar net vector, without current spread, Thick grey arrows = 40% current spread from C7/T1 electrode and resultant monaural net vector).

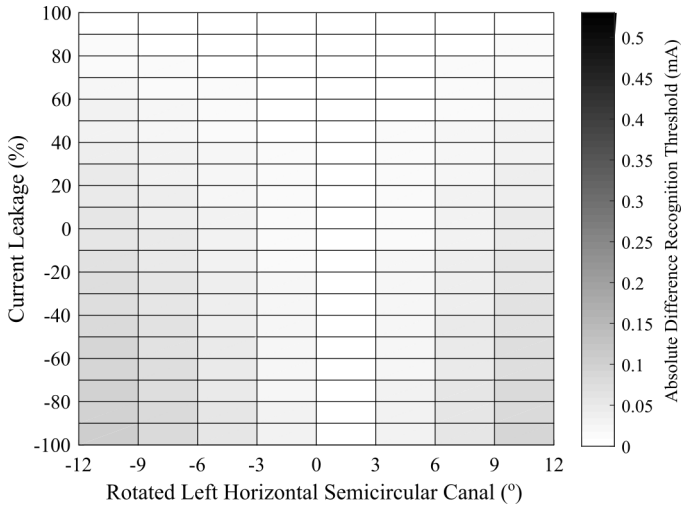

Figure 9. Grey scale map of the asymmetry in monaural recognition threshold (mA).
This grey scale map indicates the absolute difference (mA) of monaural recognition thresholds at various current spread and left horizontal semicircular canal orientations. Negative current spreading from the mastoid electrode, and positive current spreading from the C7/T1 electrode. At the most extreme current spread and canal rotation, the asymmetry could be 0.1 mA. The legend extends to 0.53mA because this is the mean AIS recognition threshold difference, none of the current spread or canal rotation combinations were equivalent to the mean difference observed in the AIS participant data.

Discussion

The purpose of this study was to investigate vestibular function and asymmetry in individuals with AIS and matched control participants. We utilized monaural bipolar EVS to activate the vestibular primary afferents unilaterally, and assess vestibular asymmetry. The results of this experiment confirmed our initial hypothesis. All individuals with AIS exhibited a larger functional vestibular asymmetry than matched control participants and participants with AIS appear to have an unilateral vestibular function that is abnormally dysfunctional (less sensitive to vestibular perception) than controls participants.

Asymmetric vestibular function to unilateral activation in participants with AIS

Unilateral vestibular stimuli were delivered using a monaural bipolar EVS configuration to evoke a perception of yaw rotation. Using unilateral vestibular stimuli, participants with AIS exhibited an absolute difference of 0.53 (0.37, 1.00) mA in their unilateral recognition thresholds, whereas control participants exhibited an absolute difference of 0.06 (0.05, 0.21) mA in their unilateral recognition thresholds.

The vestibular asymmetry in participants with AIS was related to a higher threshold response to a unilateral vestibular activation compared to healthy controls. Vestibular function for the vestibular apparatus exhibiting the lower threshold response to unilateral vestibular stimuli was similar between individuals with AIS and controls. Hence, it appears that individuals with AIS present with a unilateral peripheral vestibular system were not as sensitive as healthy controls. Using caloric vestibular stimulation, Sahlstrand et al. (1979a) reported that individuals with a right thoracic AIS exhibited an 8.6% asymmetry in their ocular response compared to a 3.7% asymmetry observed in controls. Vestibular-evoked balance responses were also more

pronounced in individuals with AIS (Sahlstrand et al., 1979b). Conversely, Hitier et al. (2015) did not observe a vestibular asymmetry in individuals with AIS also using caloric vestibular stimuli. Our results support Sahlstrand's findings but further indicate a greater vestibular asymmetry than previously reported: each AIS participant exhibited a larger vestibular asymmetry than all control participants. The larger effect size observed here may indicate that monaural EVS is a more sensitive technique than caloric vestibular stimulation to assess vestibular asymmetry. The different asymmetry magnitudes reported could be partly related to the vestibular afferents activated by caloric vestibular stimulation (lateral semicircular canal; Coats & Smith, 1967; Minor & Goldberg, 1990; Paige, 1985) vs. EVS (all vestibular afferents; (Fitzpatrick & Day, 2004; Goldberg et al., 1982) or the tested vestibular function (ocular vs. perception).

We did not observe a relationship between vestibular asymmetry and the spine curvature direction/amplitude (pre-operative Cobb's angle for AIS participants with spinal fusion surgery) in participants with AIS. When removing participants with spinal fusion surgery or using their post-operative Cobb's angle, however, a significant negative relationship was observed. Sahlstrand et al. (1979a) only correlated direction of curvature with direction of vestibular asymmetry, not the magnitude, but did not report a significant correlation. These results, may indicate the vestibular asymmetry is driven by the participant's curvature but more work is needed to confirm this.

Based on our results and predictions from our summed vector operations model, monaural EVS cannot be assumed to activate only the primary vestibular afferents from the side on which the mastoid electrode is affixed. Our data suggest that 40% of the current during monaural EVS from the C7/T1 electrode stimulates the opposite vestibular primary afferents.

This prediction is in line with the non-linear vector summation of balance and ocular responses to EVS administered in monaural and binaural configurations (Aw et al., 2013; Day et al., 2010). Based on the orientation of the semi-circular canals reported by Della Santina (2005), a 40% cross stimulation, however, cannot explain the vestibular functional asymmetry reported here. Similarly, the asymmetric semicircular canal orientation reported by Shi et al. (2011) resulted in minimal differences in the predicted recognition thresholds to monaural EVS, explaining less than 2% of the functional vestibular asymmetry observed here. Consequently, we propose the functional vestibular asymmetry observed in individuals with AIS is related to dysfunction of one vestibular apparatus and not methodological considerations associated with EVS or semi-circular canal orientation.

Vestibular function to bilateral activation in participants with AIS

The vestibular recognition thresholds of binaural bipolar EVS and real rotations were similar between control and participants with AIS. The vestibular asymmetry to unilateral vestibular stimuli seems to be, at least partly, compensated for during bilateral activation of the vestibular system (Massot et al., 2011). In monkeys, direct recordings from vestibular afferents indicated that vestibular recognition thresholds are more than likely a result of combining the activity of multiple neurons known to project to higher-order brain centers for conscious perception (Massot et al., 2011). This compensation may explain the difficulty in identifying a vestibular dysfunction in AIS using bilateral activation of vestibular afferents (Pialasse et al., 2015, Wiener-Vacher et al., 1998). These authors reported that between 50% and 67% of individuals with AIS exhibited a vestibular dysfunction, based on participant's larger sway response to vestibular evoked balance tasks. Reviewing our data, we observed that 30% of our

AIS sample demonstrated a larger vestibular recognition threshold to binaural bipolar EVS, but not in the recognition thresholds to real rotations. Hence, it is possible that with a larger sample size ($n \approx 20$/group), a significant difference in recognition threshold to binaural bipolar EVS could be detected. Even with a larger sample, there would remain a considerable overlap between the binaural recognition thresholds of participants with AIS and control participants. This would not improve the diagnostic utility of the recognition threshold to bilateral stimulation. However, given that an asymmetry in vestibular function larger than controls was observed in all participants with AIS, monaural EVS could lead to a diagnostic criterion with both a high sensitivity and specificity.

Clinical implications

Vestibular perception measurement is a simple, cost effective tool to assess vestibular function (Merfeld, 2011). Previous reports from caloric vestibular stimulation include participants not being able to tolerate the stimulation due to vertigo and nausea (Sahlstrand et al., 1979b). All of the participants in the present study tolerated the stimulus well, with all participants reporting that they enjoyed the experiment and no one reporting vertigo or nausea. As a clinical tool, a simple device could be connected to the participant and, with minimal training, an assessor could conduct a vestibular recognition threshold assessment. The methods and asymmetry metric used here could be an economical and novel way to assess scoliosis, possibly even prior to the onset of spine curvature, although this latter supposition requires testing. The results from our study are very promising, but more research needs to be done to verify these results as a prognostic tool or to develop a new modality to treat/manage scoliosis based on these findings.

Limitations of this study

The EVS methodology used here activates all the primary vestibular afferents from the semi-circular canals and otoliths. Balance responses to monaural EVS in the same head orientation suggest that there is little otolith contribution to the net movement vector, however this has not been fully assessed (Mian et al., 2010). Consequently, additional experiments targeting specifically otolithic function are required. Finally, vestibular perception represents only one domain of vestibular function and other aspects of vestibular functions, such as other components of the vestibular system, should be investigated. To assess if participants with AIS who had had spinal fusion surgery influenced the data, we completed all of the above analyses with and without the individuals with AIS who received a surgery (n = 2) and their matched control participants (n = 2). No differences between datasets including or not these individuals were observed in both vestibular recognition thresholds to unilateral or bilateral stimuli. However, the small number of participants with spinal fusion surgery does not allow us to draw any conclusions regarding the relative strength of the observed effects between participants with AIS that had spinal fusion surgery and those who have not.

Conclusion

This research supports the hypothesis that individuals with AIS have an asymmetric vestibular function that is clearly detectable with unilateral electrical vestibular stimuli. Our results suggest that vestibular dysfunction on one side in individuals with AIS, but that this functional asymmetry is compensated during bilateral activation of the vestibular system. The methods used in this research can be readily adapted for assessing vestibular function in a

clinical setting, and could potentially detect scoliosis prior to symptom onset, ideally allowing for earlier intervention and mitigation of scoliotic curvature.

Chapter 3: General discussion and future directions

General Discussion

The aim of this thesis was to assess if individuals with AIS exhibit an asymmetric vestibular function. In this study, participants with AIS had a larger vestibular asymmetry to unilateral vestibular stimuli than control participants, confirming our original hypothesis. The psychophysical methodology used in this thesis allowed for quantifying vestibular recognition threshold to compare vestibular perception of participants with AIS. Participants with AIS have more asymmetric vestibular recognition threshold to unilateral vestibular stimuli in comparison to control participants but no difference between groups in vestibular recognition threshold to bilateral vestibular stimuli was observed. Other studies also found that participants with AIS had asymmetric vestibulo-ocular and evoked balance responses to unilateral caloric vestibular stimuli (Sahlstrand et al., 1979a, 1979b). Our results are very promising because of the lack of overlap in the difference between unilateral recognition thresholds of the experimental groups. A number of considerations should be noted for future progress to understand vestibular function in individuals with AIS that could lead to early screening of scoliosis prior to visible symptoms, or potentially to a new modality involving the vestibular system to manage scoliotic curvature.

Considerations of vestibular bias

A potentially important factor that could play a role in vestibular function and functional asymmetry is vestibular bias (Merfeld, 2011). Vestibular bias is the tendency to perceive a head motion in a direction more strongly than the opposite direction, or an offset from zero (Merfeld, 2011). Vestibular bias should be considered because it could have a possible effect on vestibular

recognition threshold measurements (Merfeld, 2011)**.** Our methodology was not designed to assess vestibular bias, but, following data collection, we evaluated each participant's vestibular bias by plotting their left - right responses at a particular stimulus level and the "correctness" of their response. Participant's responses were correct 100% of the time at ± 5 mA or ± 10 ^{o}/s. If the plot intercepts the y axis at 0, it is indicative of no vestibular bias, whereas, a positive y-intercept indicates a right direction dominant vestibular bias, and a negative y-intercept indicates a left direction dominant vestibular bias. Our *post-hoc* analyses revealed that there is no vestibular bias in AIS or control participants (Figure 10). These results are corroborated by Roditi and Crane's results in healthy participants, though vestibular bias was evaluated differently (2012). During their data collection, sham trials (without vestibular stimuli) were introduced and the responses from the sham trials were used for their vestibular bias analysis. Given our results, the vestibular asymmetry reported is not likely the result of vestibular bias.

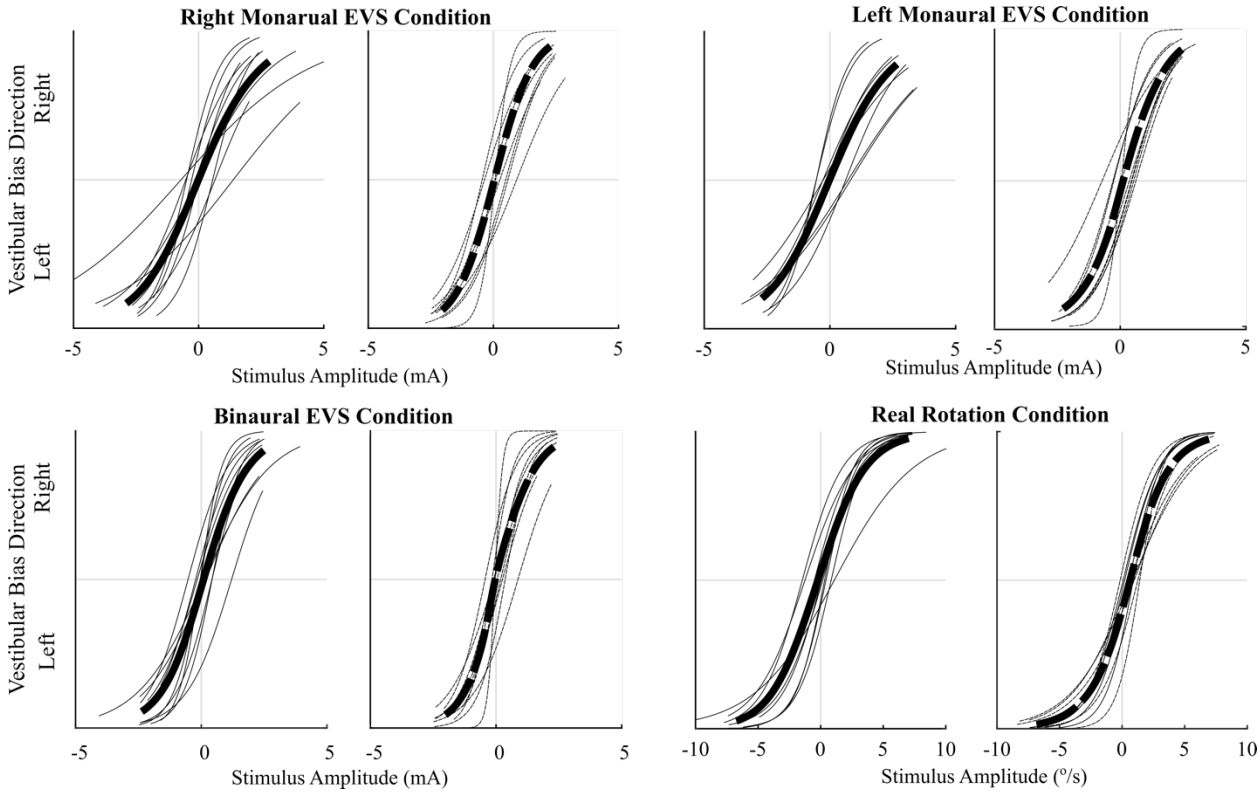

Figure 10. Pilot vestibular bias subplots

Vestibular bias plots based on Merfeld et al.'s paper (2011). Bottom left-hand corner is correct left responses and top right-hand corner is correct right responses. If the plot crosses through (0,0) then the participant has no vestibular bias. Positive y intercept values= a right dominant vestibular bias, Negative y intercept values = a left dominant vestibular bias.
(Solid line = individual AIS participant; Bold solid line = AIS mean; Dashed line = individual control participant; Bold solid line = Control mean.)

Alternative methodologies to assess vestibular asymmetry in individuals with AIS

There are alternative methodologies to stimulate the vestibular system unilaterally to assess functional vestibular asymmetry. Previous research that assessed unilateral vestibular function used caloric vestibular stimulation. However, caloric vestibular stimulation, primarily stimulates the horizontal semicircular canal afferent (Coats et al., 1967). Alternating cold (20^{o}C) and warm (50^{o}C) water or air into the external auditory canal stimulates the horizontal semicircular canal, eliciting a VOR or vestibular-evoked balance response (Coats et al., 1967; Minor et al., 1990). Caloric vestibular stimulation is limited by having two levels (hot or cold) and some participants do not tolerate the stimulation well (Sahlstrend et al., 1979). Unilateral bone vibration of the temporal fossa evokes a balance response of vestibular origin, likely primarily from otolith activation, and some semicircular canal component (Welgampola & Day, 2006). Bone vibration, however, likely activates the primary vestibular afferents bilaterally but this has not been experimentally or mathematically determined (Welgampola & Day, 2006). Finally, EVS can be used to assess VOR and balance responses. Neither unilateral EVS-evoked balance and ocular responses have been assessed in participants with AIS. The EVS-evoked responses could be important to compare to previous observations using caloric stimuli.

An alternate stimulus to activate the vestibular system unilaterally is loud clicks applied to one ear. Loud clicks (90 - 95 dB, 500 Hz tone bursts) primarily activate the saccule (Murofushi et al., 1996; Murofushi et al., 1995) and evoke short-latency ipsilateral responses in tonically activated sternomastoid muscle (Colebatch et al., 1994). At this point, unilateral otolith function has not been assessed in individuals with AIS.

Future clinical application and assessment

Currently, scoliosis is diagnosed once the spinal deformity can be measured on an x-ray, following referral to an orthopaedic surgeon. While more testing is required, vestibular perception testing could be an easily implemented clinical tool, and this research could lead to use as a screening tool for scoliosis. The electrical stimulator is portable, and by utilizing a laptop or mobile device, the psychophysical methodology could be completed within a patient assessment room at a hospital or doctor's office. An app could be developed to make the assessment more convenient.

To assess the diagnostic ability of the recognition thresholds to unilateral vestibular stimuli, the data were analysed using an ROC curve. Our methodology showed a 100% sensitivity, 100% specificity and therefore, an area under the curve equal to 1 (Figure 11). Although the results are very encouraging, more data and research are required due to our small sample size.

There are a number of future directions for this research. The critical missing link to this work is how vestibular perception asymmetry is or is not related to descending vestibular control of the thoraco-lumbar musculature. Future studies should aim to understand the underlying neuromuscular, and neurophysiological mechanisms between vestibular asymmetry and AIS. Future studies should also include a longitudinal study quantifying the vestibular recognition thresholds of many individuals with AIS and matched controls. This may strengthen the evidence presented in this thesis and increase the validity of the results. In addition, a prospective study should assess adolescents for vestibular dysfunction and observe whether the participants presenting a vestibular asymmetry develop scoliosis over time. Although a prospective study requires a lot of personnel, time, and resources, it would be worthwhile if these studies agree

with the previously reported data. In addition, the longitudinal study and prospective study could provide better asymmetry ranges for prognostic screening. Finally, a study should be designed to determine the reliability of a vestibular function intervention given that the aforementioned proposed studies indicate vestibular dysfunction would be directly related to spinal curvature development. Vestibular function interventions ideally would prevent or lessen the degree of scoliotic curvature in Individuals with AIS with vestibular asymmetry, and such interventions could include: a vestibular prosthetic, balance training, targeted EVS or other modalities.

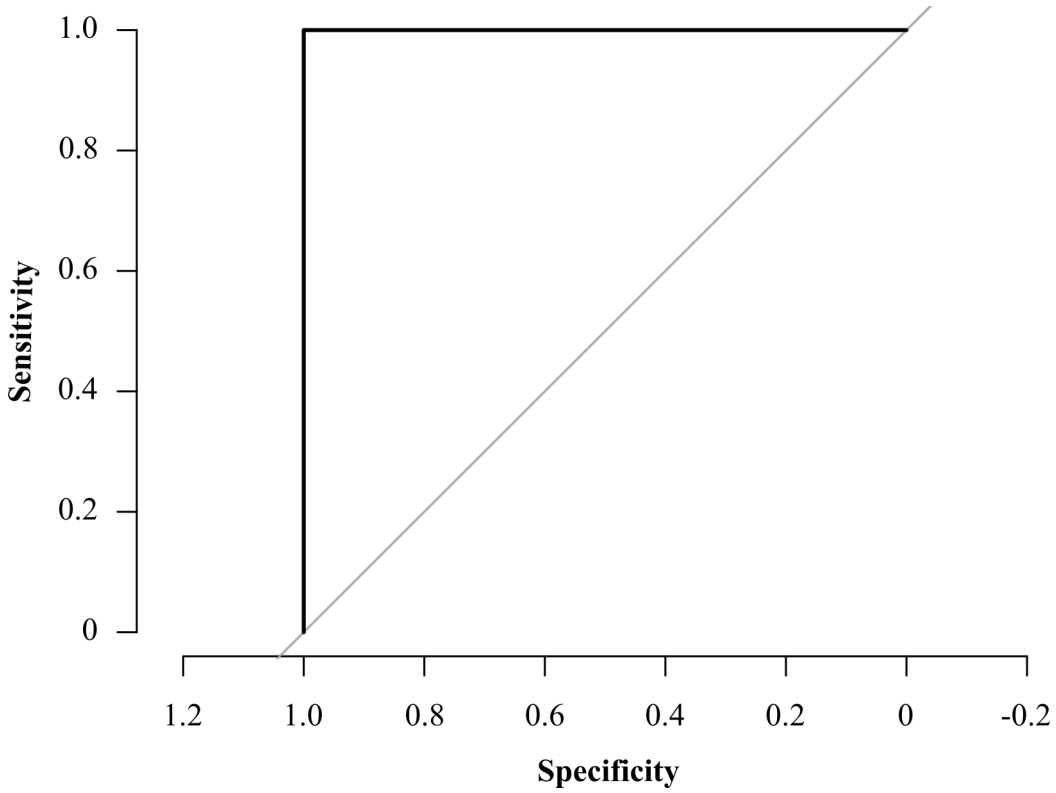

Figure 11. Receiver operating characteristics (ROC) curve.
Based on the data collected in this study, as a diagnostic test, our methodology has 100% accuracy. There was no overlap in our data, however we have a small sample size. (Area Under the Curve = 1; Sensitivity = 100%; Specificity = 100%)

Conclusion

In summary, we examined the vestibular function of adolescent idiopathic scoliotic (AIS) participants. We quantified the extent of their vestibular asymmetry based on their vestibular perception recognition thresholds to unilateral electrical vestibular stimuli. This study showed that all participants with AIS have an asymmetric vestibular function that is larger than all the control participants. Vestibular dysfunction was not detected using vestibular stimuli activating the end-organs bilaterally. This research is very promising for the future of scoliosis diagnosis and treatment, confirming the need for a greater understanding of vestibular contributions to this spinal disorder.

Work Cited

Angevine, P. D., & Deutsch, H. (2008). Idiopathic scoliosis. *Neurosurgery*, *63*(3 supplementary.), 86–93.

Aulisa, A. G., Guzzanti, V., Perisano, C., Marzetti, E., Specchia, A., Galli, M., … Koning, H. de. (2010). Determination of quality of life in adolescents with Idiopathic Scoliosis subjected to conservative treatment. *Scoliosis*, *5*(1), 21.

Aw, S. T., Todd, M. J., Lehnen, N., Aw, G. E., Weber, K. P., Eggert, T., & Halmagyi, G. M. (2013). Electrical vestibular stimulation after vestibular deafferentation and in vestibular schwannoma. *PLoS ONE*, *8*(12), 1–9.

Barrack, R. L., Whitecloud, T. S., Burke, S. W., Cook, S. D., & Harding, A. F. (1984). Proprioception in idiopathic scoliosis. *Spine*, *9*(7), 681–685.

Basaldella, E., Takeoka, A., Sigrist, M., & Arber, S. (2015). Multisensory signaling shapes vestibulo-motor circuit specificity. *Cell*, *163*, 301–312.

Bucher, S. F., Dieterich, M., Wiesmann, M., Weiss, A., Zink, R., Yousry, T. A., & Brandt, T. (1998). Cerebral functional magnetic resonance imaging of vestibular, auditory, and nociceptive areas during galvanic stimulation. *Annals of Neurology*, *44*(1), 120–125.

Byl, N. N., Holland, S., Jurek, A., & Hu, S. S. (1997). Postural imbalance and vibratory sensitivity in patients with Idiopathic Scoliosis: Implications for treatment. *Journal of Orthopaedic and Sports Physical Therapy*, *26*(2), 60–68.

Cheung, J., Veldhuizen, A. G., Halberts, J. P. K., Sluiter, W. J., & Van Horn, J. R. (2006). Geometric and electromyographic assessments in the evaluation of curve progression in Idiopathic Scoliosis. *Spine*, *31*(3), 322–329.

Coats, A. C., & Smith, S. Y. (1967). Body position and the intensity of caloric nystagmus. *Acta Oto-Laryngologica*, *63*(2–3), 515–532.

Cobb, J. (1948). Outline for the study of scolisis. Instructional course lectures. *American Academy of Orthopaedic Surgeons*, *5*, 261–275.

Colebatch, J. G., Halmagyi, G. M., & Skuse, N. F. (1994). Myogenic potentials generated by a click-evoked vestibulocollic reflex. *Journal of Neurology*, *57*, 190–197.

Cousins, S., Kaski, D., Cutfield, N., Seemungal, B., Golding, J. F., Gresty, M., … Dieterich, M. (2013). Vestibular perception following acute unilateral vestibular lesions. *PLoS ONE*, *8*(5), 1–10.

Day, B. L., Elijane, R., Welgampola, M. S., & Fitzpatrick, R. C. (2011). The human semicircular canal model of galvanic vestibular stimulation. *Experimental Brain Research*, *210*, 561–568.

Day, B. L., & Fitzpatrick, R. C. (2005). Virtual head rotation reveals a process of route reconstruction from human vestibular signals. *The Journal of Physiology*, *567*(2), 591–597.

Day, B. L., Marsden, J. F., Ramsay, E., Mian, O. S., & Fitzpatrick, R. C. (2010). Non-linear vector summation of left and right vestibular signals for human balance. *The Journal of Physiology*, *588*(4), 671–682.

Della Santina, C. C., Potyagaylo, V., Migliaccio, A. A., Minor, L. B., & Carey, J. P. (2005). Orientation of human semicircular canals measured by three-dimensional multiplanar CT reconstruction. *Journal of the Association for Research in Otolaryngology: JARO*, *6*(3), 191–206.

Donkelaar, H. J., & Boer-Van Huizen, R. (1982). Observations on the development of descending pathways from the brain stem to the spinal cord in the clawed toad Xenopus

laevis. *Anatomy and Embryology*, *163*, 461–473.
Drummond, G. B., & Tom, B. D. (2012). Presenting data: can you follow a recipe? *British Journal of Pharmacology*, *165*, 77–781.
Eatock, R. A., & Songer, J. E. (2011). Vestibular hair cells and afferents: Two channels for head motion signals. *Annual Review of Neuroscience*, *34*(1), 501–534.
Fernandez, C., & Goldberg, J. M. (1971). Physiology of peripheral neurons innervating semicircular canals of the squirrel monkey. II. Response to sinusoidal stimulation and dynamics of peripheral vestibular system. *Journal of Neurophysiology*, *34*(4), 661–675.
Fitzpatrick, R. C., & Day, B. L. (2004). Probing the human vestibular system with galvanic stimulation. *Journal of Applied Physiology*, *96*(6), 2301–2316.
Fitzpatrick, R. C., & Watson, S. R. D. (2015). Passive motion reduces vestibular balance and perceptual responses. *The Journal of Physiology*, *593*(10), 2389–2398.
Ford, D., Bagnall, K., Clements, C., & McFadden, K. (1988). Muscle spindles in the paraspinal musculature of patients with Adolescent Idiopathic Scoliosis. *Spine*, *13*(5), 461–465.
Garcia, C. D., Liu, S., Laurens, J., Deangelis, G. C., Dickman, J. D., Angelaki, D. E., & Angelaki, D. (2018). Neuronal thresholds and correlations in the peripheral vestibular system during rotation discrimination. *BioRxiv*, *1*, 1–23.
Gensberger, K. D., Kaufmann, A.-K., Dietrich, H., Branoner, F., Banchi, R., Chagnaud, B. P., & Straka, H. (2016). Galvanic vestibular stimulation: Cellular substrates and response patterns of neurons in the vestibulo-ocular network. *The Journal of Neuroscience*, *36*(35), 9097–9110.
Gescheider, G. A. (1997). *Psychophysics: The Fundamentals* (3rd ed.). Mahwah, N.J.: Lawrence Erlbaum Associates.
Goldberg, J., & Fernandez, C. (1975). Vestibular mechanisms. *Annual Review of Physiology*, *37*(1), 129–162.
Goldberg, J. M., & Cullen, K. E. (2011). Vestibular control of the head: Possible functions of the vestibulocollic reflex. *Experimental Brain Research*, *210*, 331–345.
Goldberg, J. M., Fernandez, C., & Smith, C. E. (1982). Responses of vestibular-nerve afferents in the squirrel monkey to externally applied galvanic currents. *Brain Research*, *252*(1), 156–160.
Goldberg, J. M., Smith, C. E., & Fernández, C. (1984). Relation between discharge regularity and responses to externally applied galvanic currents in vestibular nerve afferents of the squirrel monkey. *Journal of Neurophysiology*, *51*(6), 1236–1256.
Goldstein, L. A., & Waugh, T. R. (1973). Classification and terminology of Scoliosis. *Clinical Orthopaedics and Related Research*, *93*, 10–22.
Grillner, S., Hongo, T., & Lund, S. (1970). The vestibulospinal tract. Effects on alpha-motoneurones in the lumbosacral spinal cord in the cat. *Experimental Brain Research*, *10*, 94–120.
Grillner, S., Hongo, T., & Lund, S. (1971). Convergent effects on alpha motoneurones from the vestibulospinal tract and a pathway descending in the medial longitudinal fasciculus. *Experimental Brain Research*, *12*, 457–479.
Grüsser, O. J., Pause, M., & Schreiter, U. (1990). Localization and responses of neurones in the parieto-insular vestibular cortex of awake monkeys (Macaca fascicularis). *The Journal of Physiology*, *430*(1), 537–557.
Guldin, W. O., & Grüsser, O.-J. (1998). Is there a vestibular cortex? *Trends in Neuroscience*, *21*(3), 2804–2815.

Haumont, T., Gauchard, G. C., Lascombes, P., & Perrin, P. P. (2011). Postural instability in early-stage Idiopathic Scoliosis in adolescent girls. *Spine*, *36*(13), E847–E854.
Hawasli, A. H., Hullar, T. E., & Dorward, I. G. (2015). Idiopathic Scoliosis and the vestibular system. *European Spine Journal*, *24*(2), 227–233.
Herman, R., Mixon, J., Fisher, A., Maulucci, R., & Stuyck, J. (1985). Idiopathic Scoliosis and the central nervous system: A motor control problem. *Spine*, *10*(1), 1–14.
Hitier, M., Hamon, M., Denise, P., Lacoudre, J., Thenint, M.-A., Mallet, J.-F., … Quarck, G. (2015). Lateral semicircular canal asymmetry in idiopathic scoliosis: An early link between biomechanical, hormonal and neurosensory theories? *PloS One*, *10*(7), 1–20.
Huterer, M., & Cullen, K. E. (2002). Vestibulo-ocular reflex dynamics during high-frequency and high- acceleration rotations of the head on body in rhesus monkey. *Journal of Neurophysiology*, *88*(1), 13–28.
Jiang, H., Meng, Y., Jin, X., Zhang, C., Zhao, J., Wang, C., … Zhou, X. (2017). Volumetric and fatty infiltration imbalance of deep paravertebral muscles in adolescent idiopathic scoliosis. *Medical Science Monitor*, *23*, 2089–2095.
Karmali, F., Chaudhuri, S. E., Yi, Y., & Merfeld, D. M. (2016). Determining thresholds using adaptive procedures and psychometric fits: Evaluating efficiency using theory, simulations, and human experiments. *Experimental Brain Research*, *234*, 773–789.
Kim, J., & Curthoys, I. S. (2004). Responses of primary vestibular neurons to galvanic vestibular stimulation (GVS) in the anaesthetised guinea pig. *Brain Research Bulletin*, *64*, 265–271.
Konieczny, M. R., Hüsseyin, S., & Rüdiger, K. (2014). Epidemiology of Adolescent Idiopathic Scoliosis. *Journal of Child Orthopeadics*, *7*(2), 3–9.
Kontsevich, L. L., & Tyler, C. W. (1999). Bayesian adaptive estimation of psychometric slope and threshold. *Vision Research*, *16*(39), 2729–2737.
Koumbourlis, A. C. (2006). Scoliosis and the respiratory system. *Paediatric Respiratory Reviews*, *7*(1), 152–160.
Kwan, A. (2016). *Galvanic vestibular stimulation in primates: Recording vestibular afferents during transmastoid stimulation*. McGill University.
Lambert, F. M., Malinvaud, D., Glaunes, J., Bergot, C., Straka, H., & Vidal, P.-P. (2009). Vestibular asymmetry as the cause of Idiopathic Scoliosis: A possible answer from Xenopus. *Journal of Neuroscience*, *29*(40), 12477–12483.
Lowenstein, O. (1959). A functional interpretation of the electron microscopic structure of the sensory hairs in the cristae of the elamobranch, Raja clavata. *Nature*, *183*, 1807–1810.
Machida, M. (1999). Cause of idiopathic scoliosis. *Spine*, *25*(24), 2576–2583.
Mannion, A. F., Meier, M., Grob, D., & Muntener, M. (1998). Paraspinal muscle fibre type alterations associated with scoliosis: an old problem revisited with new evidence. *European Spine Journal*, *7*, 289–293.
Manzoni, D., & Miele, F. (2002). Vestibular mechanisms involved in Idiopathic Adolescent Scoliosis. *Archives Italiennes de Biologie*, (140), 67–80.
Massot, C., Chacron, M. J., & Cullen, K. E. (2011). Information transmission and detection thresholds in the vestibular nuclei: Single neurons vs. population encoding. *Journal of Neurophysiology*, *105*, 1798–1814.
Merfeld, D. M. (2011). Signal detection theory and vestibular thresholds: I. Basic theory and practical considerations. *Journal of Experimental Brain Research*, *210*(3–4), 389–405.
Mian, O. S., Dakin, C. J., Blouin, J.-S., Fitzpatrick, R. C., & Day, B. L. (2010). Lack of otolith involvement in balance responses evoked by mastoid electrical stimulation. *Journal of*

Physiology, *588*(22), 4441–4451.
Minor, L. B., & Goldberg, J. M. (1990). Influence of static head position on the horizontal nystagmus evoked by caloric, rotational and optokinetic stimulation in the squirrel monkey. *Experimental Brain Research*, *82*, 1–13.
Minor, L. B., & Goldberg, J. M. (1991). Vestibular-nerve inputs to the vestibulo-ocular reflex: A functional-ablation study in the squirrel monkey. *The Journal of Neuroscience*, *17*(6), 1636–1646.
Murofushi, T., Curthoys, I. S., & Gilchrist, D. P. (1996). Response of guinea pig vestibular nucleus neurons to clicks. *Experimental Brain Research*, *111*(1), 149–152.
Murofushi, T., Curthoys, I. S., Topple, A. N., Coleatch, J. G., & Halmagyi, G. M. (1995). Responses of guinea pig primary vestibular neurons to clicks. *Experimental Brain Research*, *103*, 174–178.
Murray, A. J., Croce, K., Belton, T., Akay, T., & Jessell, T. M. (2018). Balance control mediated by vestibular circuits directing limb extension or antagonist muscle co-activation. *Cell Reports*, *22*, 1325–1338.
Oestreich, A. E., Young, L. W., Poussaint, T. Y., Oestreich, A. E., Young, L. W., & Poussaint, T. Y. (1998). Scoliosis circa 2000: Radiologic imaging perspective I. Diagnosis and pretreatment evaluation. *Skeletal Radiolgy*, *27*, 591–605.
Paige, G. D. (1985). Caloric responses after horizontal canal inactivation. *Acta Oto-Laryngologica*, *100*(5–6), 321–327.
Patias, P., Grivas, T. B., Kaspiris, A., Aggouris, C., & Drakoutos, E. (2010). A review of the trunk surface metrics used as scoliosis and other deformities evaluation indices. *Scoliosis*, *5*(12), 1–20.
Peters, R. M., Blouin, J.-S., Dalton, B. H., & Inglis, J. T. (2016). Older adults demonstrate superior vestibular perception for virtual rotations. *Experimental Gerontology*, *82*(1), 50–57.
Peters, R. M., Rasman, B. G., Inglis, J. T., & Blouin, J.-S. (2015). Gain and phase of virtual rotation evoked by electrical vestibular stimuli. *Journal of Neurophysiology*, *114*(1), 264–273.
Petersén, I., Sahlstrand, T., & Sellden, U. (1979). Electroencephalographic Investigation of Patients with Adolescent Idiopathic Scoliosis. *Acta Orthopaedica Scandinavica*, *50*(3), 283–293.
Pettorossi, V. E., Panichi, R., Botti, F. M., Kyriakareli, A., Ferraresi, A., Faralli, M., … Bronstein, A. M. (2013). Prolonged asymmetric vestibular stimulation induces opposite, long-term effects on self-motion perception and ocular responses. *Journal of Physiology*, *591*(7), 1907–1920.
Pialasse, J.-P., Descarreaux, M., Mercier, P., Blouin, J., & Simoneau, M. (2015). The vestibular-evoked postural response of adolescents with Idiopathic Scoliosis is altered. *PloS One*, *10*(11), e0143124.
Pialasse, J.-P., Descarreaux, M., Mercier, P., & Simoneau, M. (2015). Sensory reweighting is altered in adolescent patients with scoliosis: Evidence from a neuromechanical model. *Gait and Posture*, *42*(4), 558–563.
Prowse, A., Pope, R., Gerdhem, P., & Abbott, A. (2016). Reliability and validity of inexpensive and easily administered anthropometric clinical evaluation methods of postural asymmetry measurement in Adolescent Idiopathic Scoliosis: A systematic review. *European Spine Journal*, *25*, 450–466.

Roditi, R. E., & Crane, B. T. (2012). Directional asymmetries and age effects in human self-motion perception. *Journal of the Association for Research in Otolaryngology*, *13*(3), 381–401.

Sadeghi, S. G., & Cullen, K. E. (2015). Vestibular System. In *International Encyclopedia of the Social & Behavioral Sciences* (2nd ed., pp. 63–69). Quebec: Elsevier.

Sahlstrand, T., & Petruson, B. (1979). A study of labyrinthine function in patients with adolescent idiopathic scoliosis. I. An electro-nystagmographic study. *Acta Orthopaedica Scandinavica*, *50*(6), 759–769.

Sahlstrand, T., Petruson, B., & Ortengren, R. (1979). Vestibulospinal reflex activity in patients with Adolescent Idiopathic Scoliosis: Postural effects during caloric labyrinthine stimulation recorded by stabilometry. *Acta Orthopaedica Scandinavica*, *50*(3), 275–281.

Sahlstrend, T., & Petruson, B. (1979). Postural effects on nystagmus response during caloric labyrinthine stimulation in patients with Adolescent Idiopathic Scoliosis. An electro-nystagmographic study. *Acta Orthopaedica Scandinavica*, *50*(6), 771–775.

Shi, L., Wang, D., Chu, W. C. W., Burwell, G. R., Wong, T. T., Heng, P. A., & Cheng, J. C. Y. (2011). Automatic MRI segmentation and morphoanatomy analysis of the vestibular system in Adolescent Idiopathic Scoliosis. *NeuroImage*, *54*(Supplementary 1), S180–S188.

Shotwell, S. L., Jacobs, R., & Hudspeth, A. J. (1981). Directional sensitivity of individual vertebrate hair cells to controlled deflection of their hair bundles. *Annals of the New York Academy of Sciences*, *374*(1), 1–10.

St. George, R. J., & Fitzpatrick, R. C. (2011). The sense of self-motion, orientation and balance explored by vestibular stimulation. *The Journal of Physiology*, *589*(4), 807–813.

Stetkarova, I., Zamecnik, J., Bocek, V., Vasko, P., Brabec, K., & Krbec, M. (2016). Electrophysiological and histological changes of paraspinal muscles in Adolescent Idiopathic Scoliosis. *European Spine Journal*, *25*, 3146–3153.

Suzuki, M., Kitano, H., Ito, R., Kitanishi, T., Yazawa, Y., Ogawa, T., … Kitajima, K. (2001). Cortical and subcortical vestibular response to caloric stimulation detected by functional magnetic resonance imaging. *Cognitive Brain Research*, *12*, 441–449.

Tong, J., Mao, O., & Goldreich, D. (2013). Two-point orientation discrimination versus the traditional two-point test for tactile spatial acuity assessment. *Frontier in Human Neuroscience*, *7*(579), 1–11.

Uchino, Y., Sasaki, A. M., Sato, A. H., Bai, R., & Kawamoto, A. E. (2005). Otolith and canal integration on single vestibular neurons in cats. *Experimental Brain Research*, *164*, 271–285.

Wang, W. J., Yeung, H. Y., Chu, W. C.-W., Tang, N. L.-S., Lee, K. M., Qiu, Y., … Cheng, J. C. Y. (2011). Top theories for the etiopathogenesis of Adolescent Idiopathic Scoliosis. *Journal of Pediatric Orthopaedics*, *31*(1), S14–S27.

Wardman, D. L., Taylor, J. L., & Fitzpatrick, R. C. (2003). Effects of galvanic vestibular stimulation on human posture and perception while standing. *The Journal of Physiology*, *551*(3), 1033–1042.

Welgampola, M. S., & Day, B. L. (2006). Craniocentric body-sway responses to 500 Hz bone-conducted tones in man. *Journal of Physiology*, *577*(1), 81–95.

Wiener-Vacher, S. R., & Mazda, K. (1998). Asymmetric otolith vestibulo-ocular responses in children with Idiopathic Scoliosis. *The Journal of Pediatrics*, *132*(6), 1028–1032.

Wyatt, M. P., Barrack, R. L., Mubarak, S. J., Stephen, T. S. W., & Burke, W. (1986). Vibratory response in Idiopathic Scoliosis. *The Journal of Bone and Joint Surgery*, *68*, 714–718.

Yamamoto, H., Tani, T., MacEwen, G. D., & Herman, R. (1982). An evaluation of brainstem function as a prognostication of early Idiopathic Scoliosis. *Journal of Pediatric Orthopedics*, *2*(5), 521–528.

Young, L. W., Oestreich, A. E., & Coldstein, L. A. (1970). Roentgenology in scoliosis: Contribution to evaluation and management. *American Journal of Roentgenology*, *108*(4), 778–795.

Zampieri, N., Jessell, T. M., & Murray, A. J. (2014). Mapping sensory circuits by anterograde transsynaptic transfer of recombinant Rabies virus. *Neuron*, *81*, 766–778.

Zwergal, A., Strupp, M., Brandt, T., & Büttner-Ennever, J. A. (2009). Parallel ascending vestibular pathways: Anatomical localization and functional specialization. *Annals of the New York Academy of Sciences*, *1164*, 51–59.